

# High-dimensional uncertainty estimation with sparse priors for radio interferometric imaging

Jason McEwen

[www.jasonmcewen.org](http://www.jasonmcewen.org)

@jasonmcewen

*Mullard Space Science Laboratory (MSSL)  
University College London (UCL)*

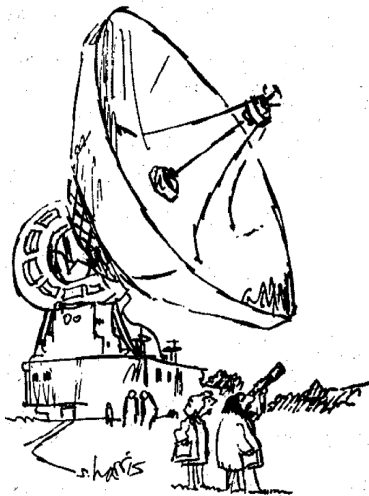
with Xiaohao Cai (MSSL) and Marcelo Pereyra (HWU)

Statistical Foundations of Uncertainty Quantification for Inverse Problems  
University of Cambridge, June 2017





# Radio telescopes are big!



“Just checking.”

# Radio telescopes are big!



# Radio interferometric telescopes

Very Large Array (VLA) in New Mexico



# Square Kilometre Array (SKA)



SPDO / Swinburne Astronomy Products

# The SKA poses a considerable big-data challenge

The SKA will use enough optical fiber to wrap twice around the Earth!

The SKA will be so sensitive that it will be able to detect an airport radar on a planet tens of light years away.

The SKA will generate enough raw data to fill 15 million 64GB iPods every day!

The dishes of the SKA will produce 10 times the global internet traffic.

The aperture arrays in the SKA could produce more than 100 times the global internet traffic.

The SKA central computer will have the processing power of about one hundred million PCs.



# Outline

- 1 Radio interferometric imaging
- 2 Proximal MCMC sampling and uncertainty quantification
- 3 MAP estimation and uncertainty quantification

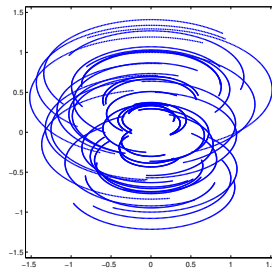
# Outline

- 1 Radio interferometric imaging
- 2 Proximal MCMC sampling and uncertainty quantification
  - Proximal Metropolis-adjusted Langevin algorithm (P-MALA)
  - Moreau-Yosida unadjusted Langevin algorithm (MYULA)
  - Numerical experiments
  - Hypothesis testing
- 3 MAP estimation and uncertainty quantification
  - Approximate local Bayesian credible intervals
  - Numerical experiments
  - Hypothesis testing

# Radio interferometric telescopes acquire "Fourier" measurements



"Fourier"  
Measurements



## Radio interferometric inverse problem

- Consider the **ill-posed inverse problem** of radio interferometric imaging:

$$\mathbf{y} = \Phi \mathbf{x} + \mathbf{n},$$

where  $\mathbf{y}$  are the measured visibilities,  $\Phi$  is the linear measurement operator,  $\mathbf{x}$  is the underlying image and  $\mathbf{n}$  is instrumental noise.

- Measurement operator, e.g.  $\Phi = \mathbf{GFA}$ , may incorporate:
  - primary beam  $\mathbf{A}$  of the telescope;
  - Fourier transform  $\mathbf{F}$ ;
  - convolutional de-gridding  $\mathbf{G}$  to interpolate to continuous  $uv$ -coordinates;
  - direction-dependent effects (DDEs)...

Interferometric imaging: recover an image from noisy and incomplete Fourier measurements.

## Radio interferometric inverse problem

- Consider the **ill-posed inverse problem** of radio interferometric imaging:

$$y = \Phi x + n,$$

where  $y$  are the measured visibilities,  $\Phi$  is the linear measurement operator,  $x$  is the underlying image and  $n$  is instrumental noise.

- Measurement operator, e.g.  $\Phi = \mathbf{GFA}$ , may incorporate:
  - primary beam  $\mathbf{A}$  of the telescope;
  - Fourier transform  $\mathbf{F}$ ;
  - convolutional de-gridding  $\mathbf{G}$  to interpolate to continuous  $uv$ -coordinates;
  - direction-dependent effects (DDEs)...

Interferometric imaging: recover an image from noisy and incomplete Fourier measurements.

## Radio interferometric inverse problem

- Consider the **ill-posed inverse problem** of radio interferometric imaging:

$$y = \Phi x + n,$$

where  $y$  are the measured visibilities,  $\Phi$  is the linear measurement operator,  $x$  is the underlying image and  $n$  is instrumental noise.

- Measurement operator, e.g.  $\Phi = \mathbf{GFA}$ , may incorporate:
  - primary beam  $\mathbf{A}$  of the telescope;
  - Fourier transform  $\mathbf{F}$ ;
  - convolutional de-gridding  $\mathbf{G}$  to interpolate to continuous  $uv$ -coordinates;
  - direction-dependent effects (DDEs)...

Interferometric imaging: recover an image from noisy and incomplete Fourier measurements.

# Sparse regularisation

## Synthesis and analysis frameworks

- Sparse **synthesis** regularisation problem:

$$\mathbf{x}_{\text{synthesis}} = \Psi \times \arg \min_{\alpha} \left[ \|\mathbf{y} - \Phi \Psi \alpha\|_2^2 + \lambda \|\alpha\|_1 \right]$$

Synthesis framework

where consider sparsifying (e.g. wavelet) representation of image:  $\mathbf{x} = \Psi \alpha$ .

- Typically sparsity assumption justified by analysing example signals in transformed domain.
- Different to synthesising signals.
- Suggests sparse **analysis** regularisation problem (Elad *et al.* 2007, Nam *et al.* 2012):

$$\mathbf{x}_{\text{analysis}} = \arg \min_{\mathbf{x}} \left[ \|\mathbf{y} - \Phi \mathbf{x}\|_2^2 + \lambda \|\Psi^\dagger \mathbf{x}\|_1 \right]$$

Analysis framework

(For orthogonal bases the two approaches are identical but otherwise very different.)

# Sparse regularisation

## Synthesis and analysis frameworks

- Sparse **synthesis** regularisation problem:

$$\mathbf{x}_{\text{synthesis}} = \Psi \times \arg \min_{\alpha} \left[ \|\mathbf{y} - \Phi \Psi \alpha\|_2^2 + \lambda \|\alpha\|_1 \right]$$

Synthesis framework

where consider sparsifying (e.g. wavelet) representation of image:  $\mathbf{x} = \Psi \alpha$ .

- Typically sparsity assumption **justified by analysing example signals** in transformed domain.
- Different to synthesising signals.**
- Suggests sparse **analysis** regularisation problem (Elad *et al.* 2007, Nam *et al.* 2012):

$$\mathbf{x}_{\text{analysis}} = \arg \min_{\mathbf{x}} \left[ \|\mathbf{y} - \Phi \mathbf{x}\|_2^2 + \lambda \|\Psi^\dagger \mathbf{x}\|_1 \right]$$

Analysis framework

(For orthogonal bases the two approaches are identical but otherwise very different.)



# Sparse regularisation

## Synthesis and analysis frameworks

- Sparse **synthesis** regularisation problem:

$$\mathbf{x}_{\text{synthesis}} = \Psi \times \arg \min_{\alpha} \left[ \|\mathbf{y} - \Phi \Psi \alpha\|_2^2 + \lambda \|\alpha\|_1 \right]$$

Synthesis framework

where consider sparsifying (e.g. wavelet) representation of image:  $\mathbf{x} = \Psi \alpha$ .

- Typically sparsity assumption **justified by analysing example signals** in transformed domain.
- Different to synthesising signals.**
- Suggests sparse **analysis** regularisation problem (Elad *et al.* 2007, Nam *et al.* 2012):

$$\mathbf{x}_{\text{analysis}} = \arg \min_{\mathbf{x}} \left[ \|\mathbf{y} - \Phi \mathbf{x}\|_2^2 + \lambda \|\Psi^\dagger \mathbf{x}\|_1 \right]$$

Analysis framework

(For **orthogonal bases** the two approaches are **identical** but otherwise very different.)

# Sparse regularisation

## SARA algorithm

- Sparsity averaging reweighted analysis (**SARA**)  
(Carrillo, McEwen & Wiaux 2012; Carrillo, McEwen, Van De Ville, Thiran & Wiaux 2013).

- Overcomplete dictionary composed of a concatenation of orthonormal bases:

$$\Psi = [\Psi_1, \Psi_2, \dots, \Psi_q]$$

with following bases: Dirac (i.e. pixel basis); Haar wavelets (promotes gradient sparsity); Daubechies wavelets two to eight  $\Rightarrow$  concatenation of 9 bases.

- Promote average sparsity by solving the constrained reweighted  $\ell_1$  analysis problem:

$$\min_{\mathbf{x} \in \mathbb{R}^N} \|\mathbf{W}\Psi^\dagger \mathbf{x}\|_1 \quad \text{subject to} \quad \|\mathbf{y} - \Phi \mathbf{x}\|_2 \leq \epsilon \quad \text{and} \quad \mathbf{x} \geq 0$$

SARA

# Sparse regularisation

## SARA algorithm

- Sparsity averaging reweighted analysis (**SARA**)  
(Carrillo, McEwen & Wiaux 2012; Carrillo, McEwen, Van De Ville, Thiran & Wiaux 2013).

- **Overcomplete dictionary** composed of a concatenation of orthonormal bases:

$$\Psi = [\Psi_1, \Psi_2, \dots, \Psi_q]$$

with following bases: **Dirac** (*i.e.* pixel basis); **Haar wavelets** (promotes gradient sparsity); **Daubechies wavelets** two to eight  $\Rightarrow$  concatenation of 9 bases.

- Promote average sparsity by solving the **constrained** reweighted  $\ell_1$  **analysis** problem:

$$\min_{\mathbf{x} \in \mathbb{R}^N} \|\mathbf{W}\Psi^\dagger \mathbf{x}\|_1 \quad \text{subject to} \quad \|\mathbf{y} - \Phi \mathbf{x}\|_2 \leq \epsilon \quad \text{and} \quad \mathbf{x} \geq 0$$

SARA

# Sparse regularisation

## SARA algorithm

- Sparsity averaging reweighted analysis (**SARA**)  
(Carrillo, McEwen & Wiaux 2012; Carrillo, McEwen, Van De Ville, Thiran & Wiaux 2013).

- **Overcomplete dictionary** composed of a concatenation of orthonormal bases:

$$\Psi = [\Psi_1, \Psi_2, \dots, \Psi_q]$$

with following bases: **Dirac** (*i.e.* pixel basis); **Haar wavelets** (promotes gradient sparsity); **Daubechies wavelets** two to eight  $\Rightarrow$  concatenation of 9 bases.

- Promote **average sparsity** by solving the **constrained** reweighted  $\ell_1$  **analysis** problem:

$$\min_{\mathbf{x} \in \mathbb{R}^N} \|\mathbf{W}\Psi^\dagger \mathbf{x}\|_1 \quad \text{subject to} \quad \|\mathbf{y} - \Phi \mathbf{x}\|_2 \leq \epsilon \quad \text{and} \quad \mathbf{x} \geq 0$$

SARA

## Distributed and parallelised convex optimisation

- Solve resulting convex optimisation problems by **proximal splitting**.
- **Block inexact ADMM algorithm** to split data and measurement operator:  
(Carrillo, McEwen & Wiaux 2014; Onose, Carrillo, Repetti, McEwen, *et al.* 2016)

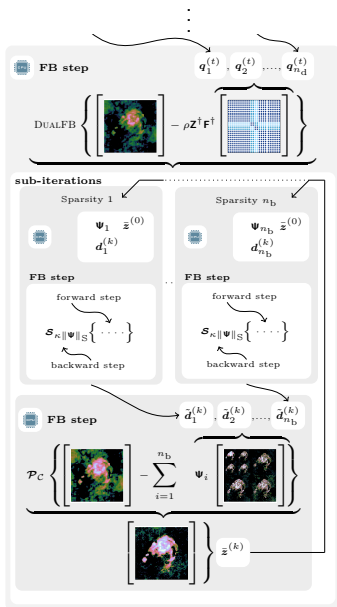
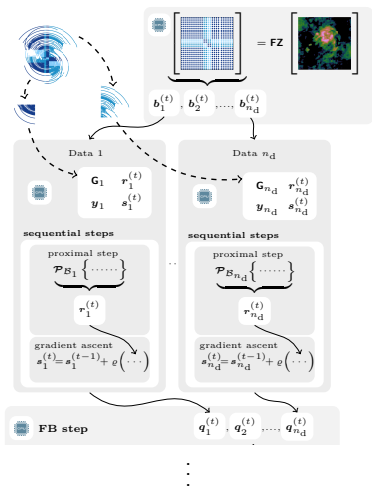
$$\mathbf{y} = \begin{bmatrix} y_1 \\ \vdots \\ y_{n_d} \end{bmatrix}, \quad \Phi = \begin{bmatrix} \Phi_1 \\ \vdots \\ \Phi_{n_d} \end{bmatrix} = \begin{bmatrix} \mathbf{G}_1 \mathbf{M}_1 \\ \vdots \\ \mathbf{G}_{n_d} \mathbf{M}_{n_d} \end{bmatrix} \mathbf{FZ}.$$

## Distributed and parallelised convex optimisation

- Solve resulting convex optimisation problems by **proximal splitting**.
- **Block inexact ADMM algorithm** to split data and measurement operator:  
(Carrillo, McEwen & Wiaux 2014; Onose, Carrillo, Repetti, McEwen, *et al.* 2016)

$$\mathbf{y} = \begin{bmatrix} \mathbf{y}_1 \\ \vdots \\ \mathbf{y}_{n_d} \end{bmatrix}, \quad \Phi = \begin{bmatrix} \Phi_1 \\ \vdots \\ \Phi_{n_d} \end{bmatrix} = \begin{bmatrix} \mathbf{G}_1 \mathbf{M}_1 \\ \vdots \\ \mathbf{G}_{n_d} \mathbf{M}_{n_d} \end{bmatrix} \mathbf{FZ}.$$

# Distributed and parallelised convex optimisation



## Public open-source codes

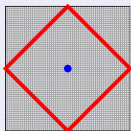
## PURIFY code

<http://basp-group.github.io/purify/>*Next-generation radio interferometric imaging*

Carrillo, McEwen, Wiaux, Pratley, d'Avezac

**PURIFY** is an open-source code that provides functionality to perform radio interferometric imaging, leveraging recent developments in the field of compressive sensing and convex optimisation.

## SOPT code

<http://basp-group.github.io/sopt/>*Sparse OPTimisation*

Carrillo, McEwen, Wiaux, Kartik, d'Avezac, Pratley, Perez-Suarez

**SOPT** is an open-source code that provides functionality to perform sparse optimisation using state-of-the-art convex optimisation algorithms.



# Imaging observations from the VLA and ATCA with PURIFY



(a) NRAO Very Large Array (VLA)



(b) Australia Telescope Compact Array (ATCA)

**Figure:** Radio interferometric telescopes considered

## PURIFY reconstruction

VLA observation of 3C129

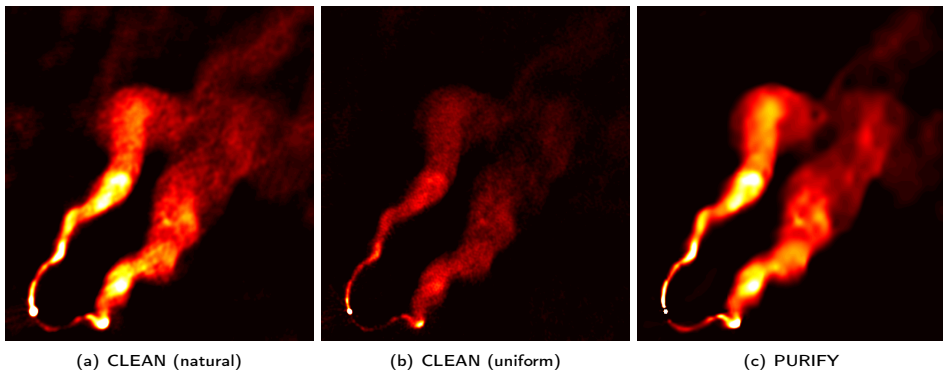
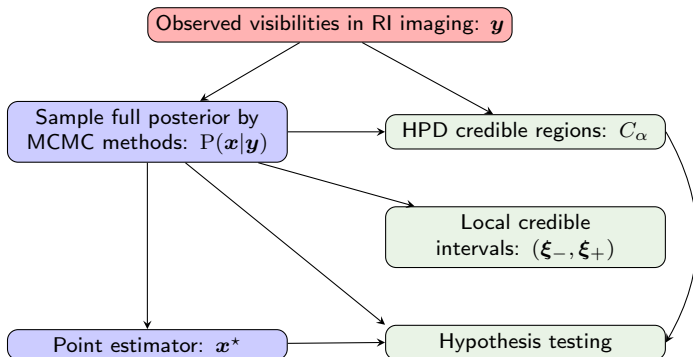


Figure: 3C129 recovered images (Pratley, McEwen, et al. 2016)

# Outline

- 1 Radio interferometric imaging
- 2 Proximal MCMC sampling and uncertainty quantification
  - Proximal Metropolis-adjusted Langevin algorithm (P-MALA)
  - Moreau-Yosida unadjusted Langevin algorithm (MYULA)
  - Numerical experiments
  - Hypothesis testing
- 3 MAP estimation and uncertainty quantification
  - Approximate local Bayesian credible intervals
  - Numerical experiments
  - Hypothesis testing

## Proximal MCMC sampling and uncertainty quantification



# Sampling the full posterior distribution

## Markov Chain Monte Carlo (MCMC)

- Sample full posterior distribution  $P(\mathbf{x} | \mathbf{y})$ .
- MCMC methods for high-dimensional problems (like interferometric imaging):
  - Gibbs sampling (sample from conditional distributions)
  - Hamiltonian MC (HMC) sampling (exploit gradients)
  - Metropolis adjusted Langevin algorithm (MALA) sampling (exploit gradients)

Require MCMC approach to support sparse priors, which shown to be highly effective.

# Sampling the full posterior distribution

## Markov Chain Monte Carlo (MCMC)

- Sample full posterior distribution  $P(\mathbf{x} | \mathbf{y})$ .
- MCMC methods for high-dimensional problems (like interferometric imaging):
  - Gibbs sampling (sample from conditional distributions)
  - Hamiltonian MC (HMC) sampling (exploit gradients)
  - Metropolis adjusted Langevin algorithm (MALA) sampling (exploit gradients)

Require MCMC approach to support sparse priors, which shown to be highly effective.

# Sampling the full posterior distribution

## Markov Chain Monte Carlo (MCMC)

- Sample full posterior distribution  $P(\mathbf{x} | \mathbf{y})$ .
- MCMC methods for high-dimensional problems (like interferometric imaging):
  - Gibbs sampling (sample from conditional distributions)
  - Hamiltonian MC (HMC) sampling (exploit gradients)
  - Metropolis adjusted Langevin algorithm (MALA) sampling (exploit gradients)

Require MCMC approach to support sparse priors, which shown to be highly effective.

# MCMC sampling with gradients

## Langevin dynamics

- Consider posteriors of the following form (and more compact notation):

$$P(\mathbf{x} | \mathbf{y}) = \underbrace{\pi(\mathbf{x})}_{\text{Posterior}} \propto \exp\left(-\underbrace{g(\mathbf{x})}_{\text{Smooth}}\right)$$

- If  $g(\mathbf{x})$  differentiable can adopt MALA (Langevin dynamics) or HMC (Hamiltonian dynamics) MCMC methods.
- Based on Langevin diffusion process  $\mathcal{L}(t)$ , with  $\pi$  as stationary distribution:

$$d\mathcal{L}(t) = \frac{1}{2} \nabla \log \pi(\mathcal{L}(t)) dt + d\mathcal{W}(t), \quad \mathcal{L}(0) = l_0$$

where  $\mathcal{W}$  is Brownian motion.

- Need gradients so cannot support sparse priors.



# MCMC sampling with gradients

## Langevin dynamics

- Consider posteriors of the following form (and more compact notation):

$$P(\mathbf{x} | \mathbf{y}) = \underbrace{\pi(\mathbf{x})}_{\text{Posterior}} \propto \exp\left(-\underbrace{g(\mathbf{x})}_{\text{Smooth}}\right)$$

- If  $g(\mathbf{x})$  differentiable can adopt MALA (Langevin dynamics) or HMC (Hamiltonian dynamics) MCMC methods.
- Based on Langevin diffusion process  $\mathcal{L}(t)$ , with  $\pi$  as stationary distribution:

$$d\mathcal{L}(t) = \frac{1}{2} \nabla \log \pi(\mathcal{L}(t)) dt + d\mathcal{W}(t), \quad \mathcal{L}(0) = l_0$$

where  $\mathcal{W}$  is Brownian motion.

- Need gradients so cannot support sparse priors.

# MCMC sampling with gradients

## Langevin dynamics

- Consider posteriors of the following form (and more compact notation):

$$P(\mathbf{x} | \mathbf{y}) = \underbrace{\pi(\mathbf{x})}_{\text{Posterior}} \propto \exp\left(-\underbrace{g(\mathbf{x})}_{\text{Smooth}}\right)$$

- If  $g(\mathbf{x})$  differentiable can adopt MALA (Langevin dynamics) or HMC (Hamiltonian dynamics) MCMC methods.
- Based on Langevin diffusion process  $\mathcal{L}(t)$ , with  $\pi$  as stationary distribution:

$$d\mathcal{L}(t) = \frac{1}{2} \nabla \log \pi(\mathcal{L}(t)) dt + d\mathcal{W}(t), \quad \mathcal{L}(0) = l_0$$

where  $\mathcal{W}$  is Brownian motion.

- Need gradients so cannot support sparse priors.

# MCMC sampling with gradients

## Langevin dynamics

- Consider posteriors of the following form (and more compact notation):

$$P(\mathbf{x} | \mathbf{y}) = \underbrace{\pi(\mathbf{x})}_{\text{Posterior}} \propto \exp\left(-\underbrace{g(\mathbf{x})}_{\text{Smooth}}\right)$$

- If  $g(\mathbf{x})$  differentiable can adopt MALA (Langevin dynamics) or HMC (Hamiltonian dynamics) MCMC methods.
- Based on Langevin diffusion process  $\mathcal{L}(t)$ , with  $\pi$  as stationary distribution:

$$d\mathcal{L}(t) = \frac{1}{2} \underbrace{\nabla \log \pi(\mathcal{L}(t))}_{\text{Gradient}} dt + d\mathcal{W}(t), \quad \mathcal{L}(0) = l_0$$

where  $\mathcal{W}$  is Brownian motion.

- Need gradients so **cannot support sparse priors**.

# Proximity operators

## A brief aside

- Define proximity operator:

$$\text{prox}_g^\lambda(\mathbf{x}) = \arg \min_{\mathbf{u}} \left[ g(\mathbf{u}) + \|\mathbf{u} - \mathbf{x}\|^2 / 2\lambda \right]$$

- Generalisation of projection operator:

$$\mathcal{P}_{\mathcal{C}}(\mathbf{x}) = \arg \min_{\mathbf{u}} \left[ \iota_{\mathcal{C}}(\mathbf{u}) + \|\mathbf{u} - \mathbf{x}\|^2 / 2 \right],$$

where  $\iota_{\mathcal{C}}(\mathbf{u}) = \infty$  if  $\mathbf{u} \notin \mathcal{C}$  and zero otherwise.

# Proximity operators

## A brief aside

- Define **proximity operator**:

$$\text{prox}_g^\lambda(\mathbf{x}) = \arg \min_{\mathbf{u}} \left[ g(\mathbf{u}) + \|\mathbf{u} - \mathbf{x}\|^2 / 2\lambda \right]$$

- Generalisation of **projection operator**:

$$\mathcal{P}_{\mathcal{C}}(\mathbf{x}) = \arg \min_{\mathbf{u}} \left[ \iota_{\mathcal{C}}(\mathbf{u}) + \|\mathbf{u} - \mathbf{x}\|^2 / 2 \right],$$

where  $\iota_{\mathcal{C}}(\mathbf{u}) = \infty$  if  $\mathbf{u} \notin \mathcal{C}$  and zero otherwise.

# Proximity operators

## A brief aside

- Define proximity operator:

$$\text{prox}_g^\lambda(\mathbf{x}) = \arg \min_{\mathbf{u}} \left[ g(\mathbf{u}) + \|\mathbf{u} - \mathbf{x}\|^2 / 2\lambda \right]$$

- Generalisation of projection operator:

$$\mathcal{P}_{\mathcal{C}}(\mathbf{x}) = \arg \min_{\mathbf{u}} \left[ \iota_{\mathcal{C}}(\mathbf{u}) + \|\mathbf{u} - \mathbf{x}\|^2 / 2 \right],$$

where  $\iota_{\mathcal{C}}(\mathbf{u}) = \infty$  if  $\mathbf{u} \notin \mathcal{C}$  and zero otherwise.

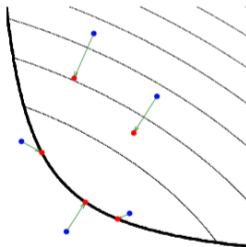


Figure: Illustration of proximity operator [Credit: Parikh & Boyd (2013)]

# Proximal MCMC methods

- Exploit proximal calculus.
- “Replace gradients with sub-gradients”.

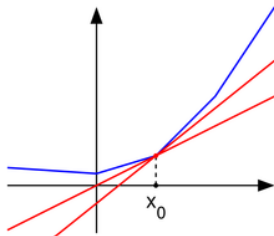


Figure: Illustration of sub-gradients [Credit: Wikipedia (Maksim)]

# Proximal MALA

## Moreau approximation

- Moreau approximation of  $f(\mathbf{x}) \propto \exp(-g(\mathbf{x}))$ :

$$f_{\lambda}^{\text{MA}}(\mathbf{x}) = \sup_{\mathbf{u} \in \mathbb{R}^N} f(\mathbf{u}) \exp\left(-\frac{\|\mathbf{u} - \mathbf{x}\|^2}{2\lambda}\right)$$

- Important properties of  $f_{\lambda}^{\text{MA}}(\mathbf{x})$ :

- As  $\lambda \rightarrow 0$ ,  $f_{\lambda}^{\text{MA}}(\mathbf{x}) \rightarrow f(\mathbf{x})$
- $\nabla \log f_{\lambda}^{\text{MA}}(\mathbf{x}) = (\text{prox}_{g/\lambda}^{\lambda}(\mathbf{x}) - \mathbf{x})/\lambda$

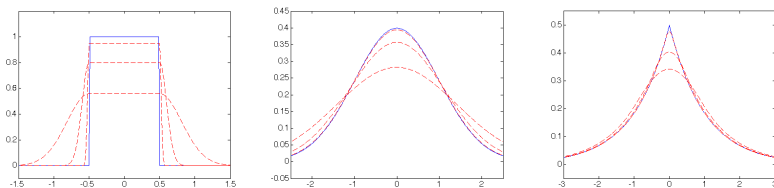


Figure: Illustration of Moreau approximations [Credit: Pereyra 2016a]



# Proximal MALA

## Moreau approximation

- Moreau approximation of  $f(\mathbf{x}) \propto \exp(-g(\mathbf{x}))$ :

$$f_{\lambda}^{\text{MA}}(\mathbf{x}) = \sup_{\mathbf{u} \in \mathbb{R}^N} f(\mathbf{u}) \exp\left(-\frac{\|\mathbf{u} - \mathbf{x}\|^2}{2\lambda}\right)$$

- Important properties of  $f_{\lambda}^{\text{MA}}(\mathbf{x})$ :

- As  $\lambda \rightarrow 0$ ,  $f_{\lambda}^{\text{MA}}(\mathbf{x}) \rightarrow f(\mathbf{x})$
- $\nabla \log f_{\lambda}^{\text{MA}}(\mathbf{x}) = (\text{prox}_{g^{\lambda}}(\mathbf{x}) - \mathbf{x})/\lambda$

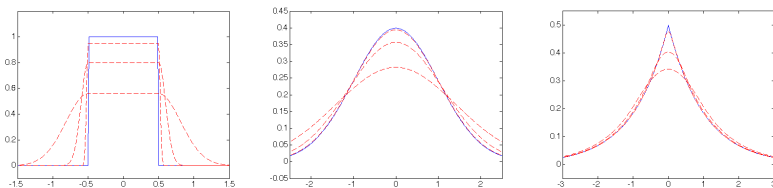


Figure: Illustration of Moreau approximations [Credit: Pereyra 2016a]

# Proximal MALA

## MCMC sampling

### Proximal Metropolis adjusted Langevin algorithm (P-MALA)

Pereyra (2016a)

- Consider log-convex posteriors:  $P(\mathbf{x} | \mathbf{y}) = \pi(\mathbf{x}) \propto \exp(-\underbrace{g(\mathbf{x})}_{\text{Convex}})$ .

- Langevin diffusion process  $\mathcal{L}(t)$ , with  $\pi$  as stationary distribution ( $\mathcal{W}$  Brownian motion):

$$d\mathcal{L}(t) = \frac{1}{2} \nabla \log \pi(\mathcal{L}(t)) dt + d\mathcal{W}(t), \quad \mathcal{L}(0) = l_0.$$

- Euler discretisation and apply Moreau approximation to  $\pi$ :

$$l^{(m+1)} = l^{(m)} + \frac{\delta}{2} \underbrace{\nabla \log \pi(l^{(m)})}_{\text{Moreau approximation}} + \sqrt{\delta} w^{(m)}.$$

$$\nabla \log \pi_{\lambda}(\mathbf{x}) = (\text{prox}_{g^{\lambda}}(\mathbf{x}) - \mathbf{x})/\lambda$$

- Metropolis-Hastings accept-reject step.

# Proximal MALA

## MCMC sampling

### Proximal Metropolis adjusted Langevin algorithm (P-MALA)

Pereyra (2016a)

- Consider log-convex posteriors:  $P(\mathbf{x} | \mathbf{y}) = \pi(\mathbf{x}) \propto \exp(-\underbrace{g(\mathbf{x})}_{\text{Convex}})$ .
- Langevin diffusion process  $\mathcal{L}(t)$ , with  $\pi$  as stationary distribution ( $\mathcal{W}$  Brownian motion):

$$d\mathcal{L}(t) = \frac{1}{2} \nabla \log \pi(\mathcal{L}(t)) dt + d\mathcal{W}(t), \quad \mathcal{L}(0) = l_0.$$

- Euler discretisation and apply Moreau approximation to  $\pi$ :

$$l^{(m+1)} = l^{(m)} + \frac{\delta}{2} \underbrace{\nabla \log \pi(l^{(m)})}_{\text{Moreau approx}} + \sqrt{\delta} w^{(m)}.$$

$$\nabla \log \pi_\lambda(\mathbf{x}) = (\text{prox}_g^\lambda(\mathbf{x}) - \mathbf{x})/\lambda$$

- Metropolis-Hastings accept-reject step.

# Proximal MALA

## MCMC sampling

### Proximal Metropolis adjusted Langevin algorithm (P-MALA)

Pereyra (2016a)

- Consider log-convex posteriors:  $P(\mathbf{x} | \mathbf{y}) = \pi(\mathbf{x}) \propto \exp(-\underbrace{g(\mathbf{x})}_{\text{Convex}})$ .
- Langevin diffusion process  $\mathcal{L}(t)$ , with  $\pi$  as stationary distribution ( $\mathcal{W}$  Brownian motion):

$$d\mathcal{L}(t) = \frac{1}{2} \nabla \log \pi(\mathcal{L}(t)) dt + d\mathcal{W}(t), \quad \mathcal{L}(0) = l_0.$$

- Euler discretisation and apply Moreau approximation to  $\pi$ :

$$\mathbf{l}^{(m+1)} = \mathbf{l}^{(m)} + \frac{\delta}{2} \underbrace{\nabla \log \pi(\mathbf{l}^{(m)})}_{\text{Moreau approximation}} + \sqrt{\delta} \mathbf{w}^{(m)}.$$

$$\nabla \log \pi_\lambda(\mathbf{x}) = (\text{prox}_g^\lambda(\mathbf{x}) - \mathbf{x})/\lambda$$

- Metropolis-Hastings accept-reject step.

# Proximal MALA

## MCMC sampling

### Proximal Metropolis adjusted Langevin algorithm (P-MALA)

Pereyra (2016a)

- Consider log-convex posteriors:  $P(\mathbf{x} | \mathbf{y}) = \pi(\mathbf{x}) \propto \exp(-\underbrace{g(\mathbf{x})}_{\text{Convex}})$ .
- Langevin diffusion process  $\mathcal{L}(t)$ , with  $\pi$  as stationary distribution ( $\mathcal{W}$  Brownian motion):

$$d\mathcal{L}(t) = \frac{1}{2} \nabla \log \pi(\mathcal{L}(t)) dt + d\mathcal{W}(t), \quad \mathcal{L}(0) = l_0.$$

- Euler discretisation and apply Moreau approximation to  $\pi$ :

$$\mathbf{l}^{(m+1)} = \mathbf{l}^{(m)} + \frac{\delta}{2} \underbrace{\nabla \log \pi(\mathbf{l}^{(m)})}_{\text{Moreau approximation}} + \sqrt{\delta} \mathbf{w}^{(m)}.$$

$$\nabla \log \pi_\lambda(\mathbf{x}) = (\text{prox}_g^\lambda(\mathbf{x}) - \mathbf{x})/\lambda$$

- Metropolis-Hastings accept-reject step.

# Proximal MALA

## Computing proximity operators for the analysis case

- Recall posterior:  $\pi(\mathbf{x}) \propto \exp(-g(\mathbf{x}))$ .

- Let  $\bar{g}(\mathbf{x}) = \bar{f}_1(\mathbf{x}) + \bar{f}_2(\mathbf{x})$ , where  $\bar{f}_1(\mathbf{x}) = \mu \|\Psi^\dagger \mathbf{x}\|_1$  and  $\bar{f}_2(\mathbf{x}) = \|\mathbf{y} - \Phi \mathbf{x}\|_2^2 / 2\sigma^2$ .

Prior

Likelihood

- Must solve an optimisation problem for each iteration!

$$\text{prox}_{\bar{g}}^{\delta/2}(\mathbf{x}) = \underset{\mathbf{u} \in \mathbb{R}^N}{\text{argmin}} \left\{ \mu \|\Psi^\dagger \mathbf{u}\|_1 + \frac{\|\mathbf{y} - \Phi \mathbf{u}\|_2^2}{2\sigma^2} + \frac{\|\mathbf{u} - \mathbf{x}\|_2^2}{\delta} \right\}.$$

- Taylor expansion at point  $\mathbf{x}$ :  $\|\mathbf{y} - \Phi \mathbf{u}\|_2^2 \approx \|\mathbf{y} - \Phi \mathbf{x}\|_2^2 + 2(\mathbf{u} - \mathbf{x})^\top \Phi^\dagger (\Phi \mathbf{x} - \mathbf{y})$ .
- Then proximity operator approximated by

$$\text{prox}_{\bar{g}}^{\delta/2}(\mathbf{x}) \approx \text{prox}_{\bar{f}_1}^{\delta/2} \left( \mathbf{x} - \delta \Phi^\dagger (\Phi \mathbf{x} - \mathbf{y}) / 2\sigma^2 \right).$$

Single forward-backward iteration

- Analytic approximation:

$$\text{prox}_{\bar{g}}^{\delta/2}(\mathbf{x}) \approx \bar{\mathbf{v}} + \Psi \left( \text{soft}_{\mu\delta/2}(\Psi^\dagger \bar{\mathbf{v}}) - \Psi^\dagger \bar{\mathbf{v}} \right), \text{ where } \bar{\mathbf{v}} = \mathbf{x} - \delta \Phi^\dagger (\Phi \mathbf{x} - \mathbf{y}) / 2\sigma^2.$$

# Proximal MALA

## Computing proximity operators for the analysis case

- Recall posterior:  $\pi(\mathbf{x}) \propto \exp(-g(\mathbf{x}))$ .

- Let  $\bar{g}(\mathbf{x}) = \bar{f}_1(\mathbf{x}) + \bar{f}_2(\mathbf{x})$ , where

$$\bar{f}_1(\mathbf{x}) = \mu \|\Psi^\dagger \mathbf{x}\|_1$$

Prior

$$\bar{f}_2(\mathbf{x}) = \|\mathbf{y} - \Phi \mathbf{x}\|_2^2 / 2\sigma^2$$

Likelihood

- Must solve an optimisation problem for each iteration!

$$\text{prox}_{\bar{g}}^{\delta/2}(\mathbf{x}) = \underset{\mathbf{u} \in \mathbb{R}^N}{\text{argmin}} \left\{ \mu \|\Psi^\dagger \mathbf{u}\|_1 + \frac{\|\mathbf{y} - \Phi \mathbf{u}\|_2^2}{2\sigma^2} + \frac{\|\mathbf{u} - \mathbf{x}\|_2^2}{\delta} \right\}$$

- Taylor expansion at point  $\mathbf{x}$ :  $\|\mathbf{y} - \Phi \mathbf{u}\|_2^2 \approx \|\mathbf{y} - \Phi \mathbf{x}\|_2^2 + 2(\mathbf{u} - \mathbf{x})^\top \Phi^\dagger (\Phi \mathbf{x} - \mathbf{y})$ .
- Then proximity operator approximated by

$$\text{prox}_{\bar{g}}^{\delta/2}(\mathbf{x}) \approx \text{prox}_{\bar{f}_1}^{\delta/2} \left( \mathbf{x} - \delta \Phi^\dagger (\Phi \mathbf{x} - \mathbf{y}) / 2\sigma^2 \right)$$

Single forward-backward iteration

- Analytic approximation:

$$\text{prox}_{\bar{g}}^{\delta/2}(\mathbf{x}) \approx \bar{\mathbf{v}} + \Psi \left( \text{soft}_{\mu\delta/2}(\Psi^\dagger \bar{\mathbf{v}}) - \Psi^\dagger \bar{\mathbf{v}} \right), \text{ where } \bar{\mathbf{v}} = \mathbf{x} - \delta \Phi^\dagger (\Phi \mathbf{x} - \mathbf{y}) / 2\sigma^2.$$

# Proximal MALA

## Computing proximity operators for the analysis case

- Recall posterior:  $\pi(\mathbf{x}) \propto \exp(-g(\mathbf{x}))$ .

- Let  $\bar{g}(\mathbf{x}) = \bar{f}_1(\mathbf{x}) + \bar{f}_2(\mathbf{x})$ , where

$$\bar{f}_1(\mathbf{x}) = \mu \|\Psi^\dagger \mathbf{x}\|_1$$

Prior

$$\bar{f}_2(\mathbf{x}) = \|\mathbf{y} - \Phi \mathbf{x}\|_2^2 / 2\sigma^2$$

Likelihood

- Must solve an optimisation problem for each iteration!

$$\text{prox}_{\bar{g}}^{\delta/2}(\mathbf{x}) = \underset{\mathbf{u} \in \mathbb{R}^N}{\text{argmin}} \left\{ \mu \|\Psi^\dagger \mathbf{u}\|_1 + \frac{\|\mathbf{y} - \Phi \mathbf{u}\|_2^2}{2\sigma^2} + \frac{\|\mathbf{u} - \mathbf{x}\|_2^2}{\delta} \right\}.$$

- Taylor expansion at point  $\mathbf{x}$ :  $\|\mathbf{y} - \Phi \mathbf{u}\|_2^2 \approx \|\mathbf{y} - \Phi \mathbf{x}\|_2^2 + 2(\mathbf{u} - \mathbf{x})^\top \Phi^\dagger (\Phi \mathbf{x} - \mathbf{y})$ .
- Then proximity operator approximated by

$$\text{prox}_{\bar{g}}^{\delta/2}(\mathbf{x}) \approx \text{prox}_{\bar{f}_1}^{\delta/2} \left( \mathbf{x} - \delta \Phi^\dagger (\Phi \mathbf{x} - \mathbf{y}) / 2\sigma^2 \right).$$

Single forward-backward iteration

- Analytic approximation:

$$\text{prox}_{\bar{g}}^{\delta/2}(\mathbf{x}) \approx \bar{\mathbf{v}} + \Psi \left( \text{soft}_{\mu\delta/2}(\Psi^\dagger \bar{\mathbf{v}}) - \Psi^\dagger \bar{\mathbf{v}} \right), \text{ where } \bar{\mathbf{v}} = \mathbf{x} - \delta \Phi^\dagger (\Phi \mathbf{x} - \mathbf{y}) / 2\sigma^2.$$



# Proximal MALA

## Computing proximity operators for the analysis case

- Recall posterior:  $\pi(\mathbf{x}) \propto \exp(-g(\mathbf{x}))$ .

- Let  $\bar{g}(\mathbf{x}) = \bar{f}_1(\mathbf{x}) + \bar{f}_2(\mathbf{x})$ , where  $\bar{f}_1(\mathbf{x}) = \mu \|\Psi^\dagger \mathbf{x}\|_1$  and  $\bar{f}_2(\mathbf{x}) = \|\mathbf{y} - \Phi \mathbf{x}\|_2^2 / 2\sigma^2$ .  
Prior Likelihood

- Must solve an optimisation problem for each iteration!

$$\text{prox}_{\bar{g}}^{\delta/2}(\mathbf{x}) = \underset{\mathbf{u} \in \mathbb{R}^N}{\text{argmin}} \left\{ \mu \|\Psi^\dagger \mathbf{u}\|_1 + \frac{\|\mathbf{y} - \Phi \mathbf{u}\|_2^2}{2\sigma^2} + \frac{\|\mathbf{u} - \mathbf{x}\|_2^2}{\delta} \right\}.$$

- Taylor expansion at point  $\mathbf{x}$ :  $\|\mathbf{y} - \Phi \mathbf{u}\|_2^2 \approx \|\mathbf{y} - \Phi \mathbf{x}\|_2^2 + 2(\mathbf{u} - \mathbf{x})^\top \Phi^\dagger (\Phi \mathbf{x} - \mathbf{y})$ .
- Then proximity operator approximated by

$$\text{prox}_{\bar{g}}^{\delta/2}(\mathbf{x}) \approx \text{prox}_{\bar{f}_1}^{\delta/2} \left( \mathbf{x} - \delta \Phi^\dagger (\Phi \mathbf{x} - \mathbf{y}) / 2\sigma^2 \right).$$

Single forward-backward iteration

- Analytic approximation:

$$\text{prox}_{\bar{g}}^{\delta/2}(\mathbf{x}) \approx \bar{\mathbf{v}} + \Psi \left( \text{soft}_{\mu\delta/2}(\Psi^\dagger \bar{\mathbf{v}}) - \Psi^\dagger \bar{\mathbf{v}} \right), \text{ where } \bar{\mathbf{v}} = \mathbf{x} - \delta \Phi^\dagger (\Phi \mathbf{x} - \mathbf{y}) / 2\sigma^2.$$

# Proximal MALA

## Computing proximity operators for the synthesis case

- Recall posterior:  $\pi(\mathbf{x}) \propto \exp(-g(\mathbf{x}))$ .
- Let  $\hat{g}(\mathbf{x}(\mathbf{a})) = \hat{f}_1(\mathbf{a}) + \hat{f}_2(\mathbf{a})$ , where  $\hat{f}_1(\mathbf{a}) = \mu \|\mathbf{a}\|_1$  and  $\hat{f}_2(\mathbf{a}) = \|\mathbf{y} - \Phi\Psi\mathbf{a}\|_2^2/2\sigma^2$ .
 

Prior
Likelihood
- Must solve an optimisation problem for each iteration!

$$\text{prox}_{\hat{g}}^{\delta/2}(\mathbf{a}) = \underset{\mathbf{u} \in \mathbb{R}^L}{\text{argmin}} \left\{ \mu \|\mathbf{u}\|_1 + \frac{\|\mathbf{y} - \Phi\Psi\mathbf{u}\|_2^2}{2\sigma^2} + \frac{\|\mathbf{u} - \mathbf{a}\|_2^2}{\delta} \right\}.$$

- Taylor expansion at point  $\mathbf{a}$ :  $\|\mathbf{y} - \Phi\Psi\mathbf{u}\|_2^2 \approx \|\mathbf{y} - \Phi\Psi\mathbf{a}\|_2^2 + 2(\mathbf{u} - \mathbf{a})^\top \Psi^\dagger \Phi^\dagger (\Phi\Psi\mathbf{a} - \mathbf{y})$ .
- Then proximity operator approximated by

$$\text{prox}_{\hat{g}}^{\delta/2}(\mathbf{a}) \approx \text{prox}_{\hat{f}_1}^{\delta/2} \left( \mathbf{a} - \delta \Psi^\dagger \Phi^\dagger (\Phi\Psi\mathbf{a} - \mathbf{y}) / 2\sigma^2 \right).$$

Single forward-backward iteration

- Analytic approximation:

$$\text{prox}_{\hat{g}}^{\delta/2}(\mathbf{a}) \approx \text{soft}_{\mu\delta/2} \left( \mathbf{a} - \delta \Psi^\dagger \Phi^\dagger (\Phi\Psi\mathbf{a} - \mathbf{y}) / 2\sigma^2 \right).$$

# Proximal MALA

## Computing proximity operators for the synthesis case

- Recall posterior:  $\pi(\mathbf{x}) \propto \exp(-g(\mathbf{x}))$ .

- Let  $\hat{g}(\mathbf{x}(\mathbf{a})) = \hat{f}_1(\mathbf{a}) + \hat{f}_2(\mathbf{a})$ , where  $\hat{f}_1(\mathbf{a}) = \mu \|\mathbf{a}\|_1$  and  $\hat{f}_2(\mathbf{a}) = \|\mathbf{y} - \Phi\Psi\mathbf{a}\|_2^2 / 2\sigma^2$ .  
Prior Likelihood

- Must solve an optimisation problem for each iteration!

$$\text{prox}_{\hat{g}}^{\delta/2}(\mathbf{a}) = \underset{\mathbf{u} \in \mathbb{R}^L}{\text{argmin}} \left\{ \mu \|\mathbf{u}\|_1 + \frac{\|\mathbf{y} - \Phi\Psi\mathbf{u}\|_2^2}{2\sigma^2} + \frac{\|\mathbf{u} - \mathbf{a}\|_2^2}{\delta} \right\}.$$

- Taylor expansion at point  $\mathbf{a}$ :  $\|\mathbf{y} - \Phi\Psi\mathbf{u}\|_2^2 \approx \|\mathbf{y} - \Phi\Psi\mathbf{a}\|_2^2 + 2(\mathbf{u} - \mathbf{a})^\top \Psi^\dagger \Phi^\dagger (\Phi\Psi\mathbf{a} - \mathbf{y})$ .
- Then proximity operator approximated by

$$\text{prox}_{\hat{g}}^{\delta/2}(\mathbf{a}) \approx \text{prox}_{\hat{f}_1}^{\delta/2} \left( \mathbf{a} - \delta \Psi^\dagger \Phi^\dagger (\Phi\Psi\mathbf{a} - \mathbf{y}) / 2\sigma^2 \right).$$

Single forward-backward iteration

- Analytic approximation:

$$\text{prox}_{\hat{g}}^{\delta/2}(\mathbf{a}) \approx \text{soft}_{\mu\delta/2} \left( \mathbf{a} - \delta \Psi^\dagger \Phi^\dagger (\Phi\Psi\mathbf{a} - \mathbf{y}) / 2\sigma^2 \right).$$

# Proximal MALA

## Computing proximity operators for the synthesis case

- Recall posterior:  $\pi(\mathbf{x}) \propto \exp(-g(\mathbf{x}))$ .

- Let  $\hat{g}(\mathbf{x}(\mathbf{a})) = \hat{f}_1(\mathbf{a}) + \hat{f}_2(\mathbf{a})$ , where  $\hat{f}_1(\mathbf{a}) = \mu \|\mathbf{a}\|_1$  and  $\hat{f}_2(\mathbf{a}) = \|\mathbf{y} - \Phi\Psi\mathbf{a}\|_2^2 / 2\sigma^2$ .  
Prior Likelihood

- Must solve an optimisation problem for each iteration!

$$\text{prox}_{\hat{g}}^{\delta/2}(\mathbf{a}) = \underset{\mathbf{u} \in \mathbb{R}^L}{\text{argmin}} \left\{ \mu \|\mathbf{u}\|_1 + \frac{\|\mathbf{y} - \Phi\Psi\mathbf{u}\|_2^2}{2\sigma^2} + \frac{\|\mathbf{u} - \mathbf{a}\|_2^2}{\delta} \right\}.$$

- Taylor expansion at point  $\mathbf{a}$ :  $\|\mathbf{y} - \Phi\Psi\mathbf{u}\|_2^2 \approx \|\mathbf{y} - \Phi\Psi\mathbf{a}\|_2^2 + 2(\mathbf{u} - \mathbf{a})^\top \Psi^\dagger \Phi^\dagger (\Phi\Psi\mathbf{a} - \mathbf{y})$ .
- Then proximity operator approximated by

$$\text{prox}_{\hat{g}}^{\delta/2}(\mathbf{a}) \approx \text{prox}_{\hat{f}_1}^{\delta/2} \left( \mathbf{a} - \delta \Psi^\dagger \Phi^\dagger (\Phi\Psi\mathbf{a} - \mathbf{y}) / 2\sigma^2 \right).$$

Single forward-backward iteration

- Analytic approximation:

$$\text{prox}_{\hat{g}}^{\delta/2}(\mathbf{a}) \approx \text{soft}_{\mu\delta/2} \left( \mathbf{a} - \delta \Psi^\dagger \Phi^\dagger (\Phi\Psi\mathbf{a} - \mathbf{y}) / 2\sigma^2 \right).$$

# Proximal MALA

## Computing proximity operators for the synthesis case

- Recall posterior:  $\pi(\mathbf{x}) \propto \exp(-g(\mathbf{x}))$ .

- Let  $\hat{g}(\mathbf{x}(\mathbf{a})) = \hat{f}_1(\mathbf{a}) + \hat{f}_2(\mathbf{a})$ , where  $\hat{f}_1(\mathbf{a}) = \mu \|\mathbf{a}\|_1$  and  $\hat{f}_2(\mathbf{a}) = \|\mathbf{y} - \Phi\Psi\mathbf{a}\|_2^2 / 2\sigma^2$ .  
 Prior Likelihood

- Must solve an optimisation problem for each iteration!

$$\text{prox}_{\hat{g}}^{\delta/2}(\mathbf{a}) = \underset{\mathbf{u} \in \mathbb{R}^L}{\text{argmin}} \left\{ \mu \|\mathbf{u}\|_1 + \frac{\|\mathbf{y} - \Phi\Psi\mathbf{u}\|_2^2}{2\sigma^2} + \frac{\|\mathbf{u} - \mathbf{a}\|_2^2}{\delta} \right\}.$$

- Taylor expansion at point  $\mathbf{a}$ :  $\|\mathbf{y} - \Phi\Psi\mathbf{u}\|_2^2 \approx \|\mathbf{y} - \Phi\Psi\mathbf{a}\|_2^2 + 2(\mathbf{u} - \mathbf{a})^\top \Psi^\dagger \Phi^\dagger (\Phi\Psi\mathbf{a} - \mathbf{y})$ .
- Then proximity operator approximated by

$$\text{prox}_{\hat{g}}^{\delta/2}(\mathbf{a}) \approx \text{prox}_{\hat{f}_1}^{\delta/2} \left( \mathbf{a} - \delta \Psi^\dagger \Phi^\dagger (\Phi\Psi\mathbf{a} - \mathbf{y}) / 2\sigma^2 \right).$$

Single forward-backward iteration

- Analytic approximation:

$$\text{prox}_{\hat{g}}^{\delta/2}(\mathbf{a}) \approx \text{soft}_{\mu\delta/2} \left( \mathbf{a} - \delta \Psi^\dagger \Phi^\dagger (\Phi\Psi\mathbf{a} - \mathbf{y}) / 2\sigma^2 \right).$$

# MYULA

## Moreau-Yosida approximation

- Moreau-Yosida approximation (Moreau envelope) of  $f$ :

$$f_\lambda^{\text{MY}}(\mathbf{x}) = \inf_{\mathbf{u} \in \mathbb{R}^N} f(\mathbf{u}) + \frac{\|\mathbf{u} - \mathbf{x}\|^2}{2\lambda}$$

- Important properties of  $f_\lambda^{\text{MY}}(\mathbf{x})$ :

- ① As  $\lambda \rightarrow 0$ ,  $f_\lambda^{\text{MY}}(\mathbf{x}) \rightarrow f(\mathbf{x})$
- ②  $\nabla f_\lambda^{\text{MY}}(\mathbf{x}) = (\mathbf{x} - \text{prox}_f^\lambda(\mathbf{x}))/\lambda$

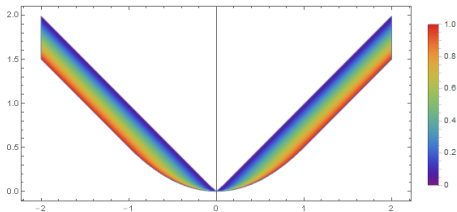


Figure: Illustration of Moreau-Yosida envelope of  $|x|$  for varying  $\lambda$  [Credit: Stack exchange (ubpdqn)]

# MYULA

## Moreau-Yosida approximation

- Moreau-Yosida approximation (Moreau envelope) of  $f$ :

$$f_\lambda^{\text{MY}}(\mathbf{x}) = \inf_{\mathbf{u} \in \mathbb{R}^N} f(\mathbf{u}) + \frac{\|\mathbf{u} - \mathbf{x}\|^2}{2\lambda}$$

- Important properties of  $f_\lambda^{\text{MY}}(\mathbf{x})$ :
  - 1 As  $\lambda \rightarrow 0$ ,  $f_\lambda^{\text{MY}}(\mathbf{x}) \rightarrow f(\mathbf{x})$
  - 2  $\nabla f_\lambda^{\text{MY}}(\mathbf{x}) = (\mathbf{x} - \text{prox}_f^\lambda(\mathbf{x}))/\lambda$

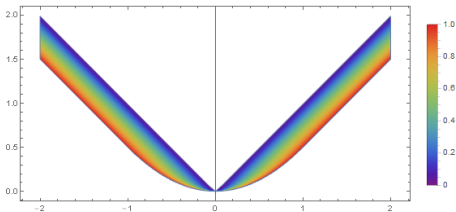


Figure: Illustration of Moreau-Yosida envelope of  $|x|$  for varying  $\lambda$  [Credit: Stack exchange (ubpdqn)]

## MYULA

## MCMC sampling

## Moreau-Yosida unadjusted Langevin algorithm (MYULA)

Durmus, Moulines &amp; Pereyra (2016)

- Consider log-convex posteriors:  $P(\mathbf{x} | \mathbf{y}) = \pi(\mathbf{x}) \propto \exp(-g(\mathbf{x}))$ , where

$$g(\mathbf{x}) = \boxed{f_1(\mathbf{x})}^{\text{Convex}} + \boxed{f_2(\mathbf{x})}^{\text{Smooth}}.$$

- Langevin diffusion process  $\mathcal{L}(t)$ , with  $\pi$  as stationary distribution ( $\mathcal{W}$  Brownian motion):

$$d\mathcal{L}(t) = \frac{1}{2} \nabla \log \pi(\mathcal{L}(t)) dt + d\mathcal{W}(t), \quad \mathcal{L}(0) = l_0.$$

- Euler discretisation and apply Moreau-Yosida approximation to  $f_1$ :

$$l^{(m+1)} = l^{(m)} + \frac{\delta}{2} \boxed{\nabla \log \pi(l^{(m)})} + \sqrt{\delta} w^{(m)}.$$

$$\nabla \log \pi(\mathbf{x}) \approx (\text{prox}_{f_1}^\lambda(\mathbf{x}) - \mathbf{x})/\lambda - \nabla f_2(\mathbf{x})$$

- No Metropolis-Hastings accept-reject step. Converges geometrically fast, where bias can be made arbitrarily small. To achieve precision target  $\epsilon$  requires:
  - Worst case: order  $N^5 \log^2(\epsilon^{-1}) \epsilon^{-2}$  iterations.
  - Strong convexity worst case: order  $N \log(N) \log^2(\epsilon^{-1}) \epsilon^{-2}$  iterations.



# MYULA

## MCMC sampling

### Moreau-Yosida unadjusted Langevin algorithm (MYULA)

Durmus, Moulines & Pereyra (2016)

- Consider log-convex posteriors:  $P(\mathbf{x} | \mathbf{y}) = \pi(\mathbf{x}) \propto \exp(-g(\mathbf{x}))$ , where

$$g(\mathbf{x}) = \boxed{f_1(\mathbf{x})}^{\text{Convex}} + \boxed{f_2(\mathbf{x})}^{\text{Smooth}}.$$

- Langevin diffusion process  $\mathcal{L}(t)$ , with  $\pi$  as stationary distribution ( $\mathcal{W}$  Brownian motion):

$$d\mathcal{L}(t) = \frac{1}{2} \nabla \log \pi(\mathcal{L}(t)) dt + d\mathcal{W}(t), \quad \mathcal{L}(0) = l_0.$$

- Euler discretisation and apply Moreau-Yosida approximation to  $f_1$ :

$$l^{(m+1)} = l^{(m)} + \frac{\delta}{2} \boxed{\nabla \log \pi(l^{(m)})} + \sqrt{\delta} w^{(m)}.$$

$$\nabla \log \pi(\mathbf{x}) \approx (\text{prox}_{f_1}^\lambda(\mathbf{x}) - \mathbf{x})/\lambda - \nabla f_2(\mathbf{x})$$

- No Metropolis-Hastings accept-reject step. Converges geometrically fast, where bias can be made arbitrarily small. To achieve precision target  $\epsilon$  requires:
  - Worst case: order  $N^5 \log^2(\epsilon^{-1}) \epsilon^{-2}$  iterations.
  - Strong convexity worst case: order  $N \log(N) \log^2(\epsilon^{-1}) \epsilon^{-2}$  iterations.

# MYULA

## MCMC sampling

### Moreau-Yosida unadjusted Langevin algorithm (MYULA)

Durmus, Moulines & Pereyra (2016)

- Consider log-convex posteriors:  $P(\mathbf{x} | \mathbf{y}) = \pi(\mathbf{x}) \propto \exp(-g(\mathbf{x}))$ , where

$$g(\mathbf{x}) = \boxed{f_1(\mathbf{x})}^{\text{Convex}} + \boxed{f_2(\mathbf{x})}^{\text{Smooth}}.$$

- Langevin diffusion process  $\mathcal{L}(t)$ , with  $\pi$  as stationary distribution ( $\mathcal{W}$  Brownian motion):

$$d\mathcal{L}(t) = \frac{1}{2} \nabla \log \pi(\mathcal{L}(t)) dt + d\mathcal{W}(t), \quad \mathcal{L}(0) = l_0.$$

- Euler discretisation and apply **Moreau-Yosida approximation to  $f_1$** :

$$\mathbf{l}^{(m+1)} = \mathbf{l}^{(m)} + \frac{\delta}{2} \boxed{\nabla \log \pi(\mathbf{l}^{(m)})} + \sqrt{\delta} \mathbf{w}^{(m)}.$$

$$\nabla \log \pi(\mathbf{x}) \approx (\text{prox}_{f_1}^\lambda(\mathbf{x}) - \mathbf{x})/\lambda - \nabla f_2(\mathbf{x})$$

- No Metropolis-Hastings accept-reject step. Converges geometrically fast, where bias can be made arbitrarily small. To achieve precision target  $\epsilon$  requires:
  - Worst case: order  $N^5 \log^2(\epsilon^{-1}) \epsilon^{-2}$  iterations.
  - Strong convexity worst case: order  $N \log(N) \log^2(\epsilon^{-1}) \epsilon^{-2}$  iterations.

# MYULA

## MCMC sampling

### Moreau-Yosida unadjusted Langevin algorithm (MYULA)

Durmus, Moulines & Pereyra (2016)

- Consider log-convex posteriors:  $P(\mathbf{x} | \mathbf{y}) = \pi(\mathbf{x}) \propto \exp(-g(\mathbf{x}))$ , where

$$g(\mathbf{x}) = \boxed{f_1(\mathbf{x})}^{\text{Convex}} + \boxed{f_2(\mathbf{x})}^{\text{Smooth}}.$$

- Langevin diffusion process  $\mathcal{L}(t)$ , with  $\pi$  as stationary distribution ( $\mathcal{W}$  Brownian motion):

$$d\mathcal{L}(t) = \frac{1}{2} \nabla \log \pi(\mathcal{L}(t)) dt + d\mathcal{W}(t), \quad \mathcal{L}(0) = l_0.$$

- Euler discretisation and apply **Moreau-Yosida approximation to  $f_1$** :

$$\mathbf{l}^{(m+1)} = \mathbf{l}^{(m)} + \frac{\delta}{2} \boxed{\nabla \log \pi(\mathbf{l}^{(m)})} + \sqrt{\delta} \mathbf{w}^{(m)}.$$

$$\nabla \log \pi(\mathbf{x}) \approx (\text{prox}_{f_1}^\lambda(\mathbf{x}) - \mathbf{x}) / \lambda - \nabla f_2(\mathbf{x})$$

- No** Metropolis-Hastings accept-reject step. Converges geometrically fast, where bias can be made arbitrarily small. To achieve precision target  $\epsilon$  requires:
  - Worst case: order  $N^5 \log^2(\epsilon^{-1}) \epsilon^{-2}$  iterations.
  - Strong convexity worst case: order  $N \log(N) \log^2(\epsilon^{-1}) \epsilon^{-2}$  iterations.

# MYULA

## Computing proximity operators for the analysis case

- Recall posterior:  $\pi(\mathbf{x}) \propto \exp(-g(\mathbf{x}))$ .
- Let  $\bar{g}(\mathbf{x}) = \bar{f}_1(\mathbf{x}) + \bar{f}_2(\mathbf{x})$ , where  $\bar{f}_1(\mathbf{x}) = \mu \|\Psi^\dagger \mathbf{x}\|_1$  and  $\bar{f}_2(\mathbf{x}) = \|\mathbf{y} - \Phi \mathbf{x}\|_2^2 / 2\sigma^2$ .
 

Prior
Likelihood
- Only need to compute proximity operator of  $f_1$ , which can be computed analytically without any approximation:

$$\text{prox}_{\bar{f}_1}^{\delta/2}(\mathbf{x}) = \mathbf{x} + \Psi \left( \text{soft}_{\mu\delta/2}(\Psi^\dagger \mathbf{x}) - \Psi^\dagger \mathbf{x} \right).$$

# MYULA

## Computing proximity operators for the analysis case

- Recall posterior:  $\pi(\mathbf{x}) \propto \exp(-g(\mathbf{x}))$ .
- Let  $\bar{g}(\mathbf{x}) = \bar{f}_1(\mathbf{x}) + \bar{f}_2(\mathbf{x})$ , where  $\bar{f}_1(\mathbf{x}) = \mu \|\Psi^\dagger \mathbf{x}\|_1$  and  $\bar{f}_2(\mathbf{x}) = \|\mathbf{y} - \Phi \mathbf{x}\|_2^2 / 2\sigma^2$ .  

Prior
Likelihood
- Only need to compute proximity operator of  $f_1$ , which can be **computed analytically without any approximation**:

$$\text{prox}_{\bar{f}_1}^{\delta/2}(\mathbf{x}) = \mathbf{x} + \Psi \left( \text{soft}_{\mu\delta/2}(\Psi^\dagger \mathbf{x}) - \Psi^\dagger \mathbf{x} \right).$$

# MYULA

## Computing proximity operators for the synthesis case

- Recall posterior:  $\pi(\mathbf{x}) \propto \exp(-g(\mathbf{x}))$ .
- Let  $\hat{g}(\mathbf{x}(\mathbf{a})) = \hat{f}_1(\mathbf{a}) + \hat{f}_2(\mathbf{a})$ , where  $\hat{f}_1(\mathbf{a}) = \mu \|\mathbf{a}\|_1$  and  $\hat{f}_2(\mathbf{a}) = \|\mathbf{y} - \Phi \Psi \mathbf{a}\|_2^2 / 2\sigma^2$ .  
 Prior Likelihood
- Only need to compute proximity operator of  $f_1$ , which can be computed analytically without any approximation:

$$\text{prox}_{\hat{f}_1}^{\delta/2}(\mathbf{a}) = \text{soft}_{\mu\delta/2}(\mathbf{a}) .$$

# MYULA

## Computing proximity operators for the synthesis case

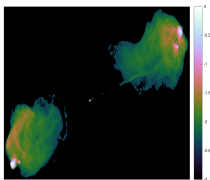
- Recall posterior:  $\pi(\mathbf{x}) \propto \exp(-g(\mathbf{x}))$ .
- Let  $\hat{g}(\mathbf{x}(\mathbf{a})) = \hat{f}_1(\mathbf{a}) + \hat{f}_2(\mathbf{a})$ , where  $\hat{f}_1(\mathbf{a}) = \mu \|\mathbf{a}\|_1$  and  $\hat{f}_2(\mathbf{a}) = \|\mathbf{y} - \Phi \Psi \mathbf{a}\|_2^2 / 2\sigma^2$ .  

Prior
Likelihood
- Only need to compute proximity operator of  $f_1$ , which can be **computed analytically without any approximation**:

$$\text{prox}_{\hat{f}_1}^{\delta/2}(\mathbf{a}) = \text{soft}_{\mu\delta/2}(\mathbf{a}) .$$

# Numerical experiments

## MYULA with analysis model



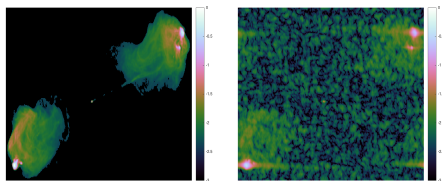
(a) Ground truth

Figure: Cygnus A



# Numerical experiments

## MYULA with analysis model



(a) Ground truth

(b) Dirty image

Figure: Cygnus A

# Numerical experiments

## MYULA with analysis model

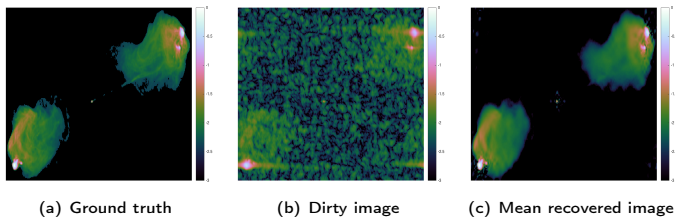


Figure: Cygnus A

# Numerical experiments

## MYULA with analysis model

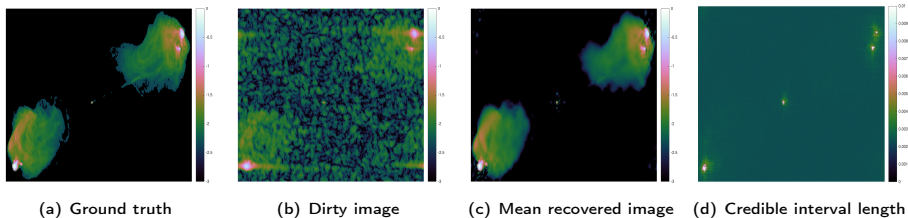


Figure: Cygnus A

# Numerical experiments

## MYULA with analysis model

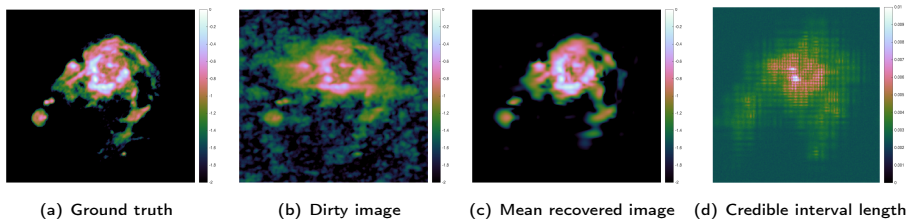


Figure: HII region of M31

# Numerical experiments

## MYULA with analysis model

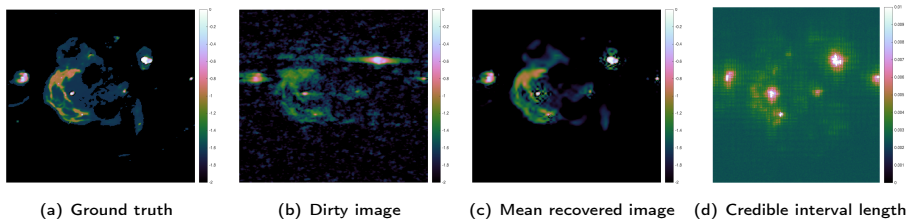


Figure: W28 Supernova remnant

# Numerical experiments

## MYULA with analysis model

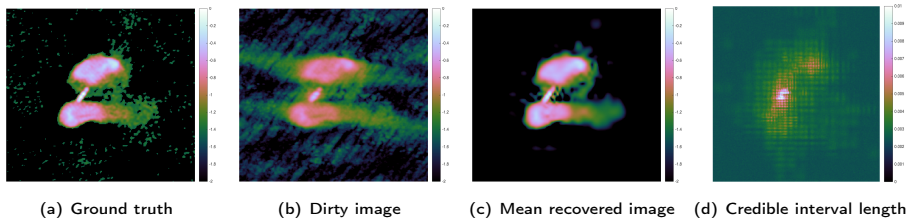


Figure: 3C288

# Numerical experiments

## Computation time

Table: CPU time in minutes for Proximal MCMC sampling

Image	Method	CPU time (min)	
		Analysis	Synthesis
Cygnus A	P-MALA	2274	1762
	MYULA	1056	942
M31	P-MALA	1307	944
	MYULA	618	581
W28	P-MALA	1122	879
	MYULA	646	598
3C288	P-MALA	1144	881
	MYULA	607	538

# Hypothesis testing

## Method

- Is structure in an image **physical or an artifact?**
- Perform **hypothesis tests** using Bayesian credible regions (Pereyra 2016b).
- Let  $C_\alpha$  denote the **highest posterior density (HPD) Bayesian credible region** with confidence level  $(1 - \alpha)\%$  defined by posterior iso-contour:  $C_\alpha = \{x : g(x) \leq \gamma_\alpha\}$ .

### Hypothesis testing of physical structure

- Cut out region containing structure of interest from recovered image  $x^*$ .
- Inpaint background (noise) into region, yielding surrogate image  $x'$ .
- Test whether  $x' \in C_\alpha$ :
  - If  $x' \in C_\alpha$ , then reject hypothesis that structure is an artifact with confidence  $(1 - \alpha)\%$ .
  - If  $x' \notin C_\alpha$ , insufficient evidence to draw conclusions about the physical nature of the structure.



# Hypothesis testing

## Method

- Is structure in an image **physical or an artifact?**
- Perform **hypothesis tests** using Bayesian credible regions (Pereyra 2016b).
- Let  $C_\alpha$  denote the highest posterior density (HPD) Bayesian credible region with confidence level  $(1 - \alpha)\%$  defined by posterior iso-contour:  $C_\alpha = \{x : g(x) \leq \gamma_\alpha\}$ .

### Hypothesis testing of physical structure

- Cut out region containing structure of interest from recovered image  $x^*$ .
- Inpaint background (noise) into region, yielding surrogate image  $x'$ .
- Test whether  $x' \in C_\alpha$ :
  - If  $x' \in C_\alpha$ , then reject hypothesis that structure is an artifact with confidence  $(1 - \alpha)\%$ .
  - If  $x' \notin C_\alpha$ , conclude that structure is an artifact with confidence  $(1 - \alpha)\%$ .

# Hypothesis testing

## Method

- Is structure in an image **physical or an artifact?**
- Perform **hypothesis tests** using Bayesian credible regions (Pereyra 2016b).
- Let  $C_\alpha$  denote the **highest posterior density (HPD) Bayesian credible region** with confidence level  $(1 - \alpha)\%$  defined by posterior iso-contour:  $C_\alpha = \{\mathbf{x} : g(\mathbf{x}) \leq \gamma_\alpha\}$ .

### Hypothesis testing of physical structure

- Cut out region containing structure of interest from recovered image  $\hat{\mathbf{x}}^*$ .
- Inpaint background (noise) into region, yielding surrogate image  $\hat{\mathbf{x}}'$ .
- Test whether  $\hat{\mathbf{x}}' \in C_\alpha$ :

• If  $\hat{\mathbf{x}}' \in C_\alpha$ , then region contains structure that is likely to be physical with confidence

• If  $\hat{\mathbf{x}}' \notin C_\alpha$ , then region contains structure that is likely to be an artifact with confidence

# Hypothesis testing

## Method

- Is structure in an image **physical or an artifact**?
- Perform **hypothesis tests** using Bayesian credible regions (Pereyra 2016b).
- Let  $C_\alpha$  denote the **highest posterior density (HPD) Bayesian credible region** with confidence level  $(1 - \alpha)\%$  defined by posterior iso-contour:  $C_\alpha = \{\mathbf{x} : g(\mathbf{x}) \leq \gamma_\alpha\}$ .

### Hypothesis testing of physical structure

- 1 Cut out region containing structure of interest from recovered image  $\mathbf{x}^*$ .
- 2 Inpaint background (noise) into region, yielding surrogate image  $\mathbf{x}'$ .
- 3 Test whether  $\mathbf{x}' \in C_\alpha$ :
  - If  $\mathbf{x}' \notin C_\alpha$  then reject hypothesis that structure is an artifact with confidence  $(1 - \alpha)\%$ , *i.e.* structure most likely physical.
  - If  $\mathbf{x}' \in C_\alpha$  uncertainty too high to draw strong conclusions about the physical nature of the structure.

# Hypothesis testing

## Method

- Is structure in an image **physical or an artifact**?
- Perform **hypothesis tests** using Bayesian credible regions (Pereyra 2016b).
- Let  $C_\alpha$  denote the **highest posterior density (HPD) Bayesian credible region** with confidence level  $(1 - \alpha)\%$  defined by posterior iso-contour:  $C_\alpha = \{\mathbf{x} : g(\mathbf{x}) \leq \gamma_\alpha\}$ .

### Hypothesis testing of physical structure

- 1 Cut out region containing structure of interest from recovered image  $\mathbf{x}^*$ .
- 2 Inpaint background (noise) into region, yielding surrogate image  $\mathbf{x}'$ .
- 3 Test whether  $\mathbf{x}' \in C_\alpha$ :
  - If  $\mathbf{x}' \notin C_\alpha$  then reject hypothesis that structure is an artifact with confidence  $(1 - \alpha)\%$ , *i.e.* structure most likely physical.
  - If  $\mathbf{x}' \in C_\alpha$  uncertainty too high to draw strong conclusions about the physical nature of the structure.

# Hypothesis testing

## Method

- Is structure in an image **physical or an artifact**?
- Perform **hypothesis tests** using Bayesian credible regions (Pereyra 2016b).
- Let  $C_\alpha$  denote the **highest posterior density (HPD) Bayesian credible region** with confidence level  $(1 - \alpha)\%$  defined by posterior iso-contour:  $C_\alpha = \{\mathbf{x} : g(\mathbf{x}) \leq \gamma_\alpha\}$ .

### Hypothesis testing of physical structure

- 1 Cut out region containing structure of interest from recovered image  $\mathbf{x}^*$ .
- 2 Inpaint background (noise) into region, yielding surrogate image  $\mathbf{x}'$ .
- 3 Test whether  $\mathbf{x}' \in C_\alpha$ :
  - If  $\mathbf{x}' \notin C_\alpha$  then reject hypothesis that structure is an artifact with confidence  $(1 - \alpha)\%$ , *i.e.* **structure most likely physical**.
  - If  $\mathbf{x}' \in C_\alpha$  uncertainty too high to draw strong conclusions about the physical nature of the structure.

# Hypothesis testing

## Method

- Is structure in an image **physical or an artifact**?
- Perform **hypothesis tests** using Bayesian credible regions (Pereyra 2016b).
- Let  $C_\alpha$  denote the **highest posterior density (HPD) Bayesian credible region** with confidence level  $(1 - \alpha)\%$  defined by posterior iso-contour:  $C_\alpha = \{\mathbf{x} : g(\mathbf{x}) \leq \gamma_\alpha\}$ .

### Hypothesis testing of physical structure

- 1 Cut out region containing structure of interest from recovered image  $\mathbf{x}^*$ .
- 2 Inpaint background (noise) into region, yielding surrogate image  $\mathbf{x}'$ .
- 3 Test whether  $\mathbf{x}' \in C_\alpha$ :
  - If  $\mathbf{x}' \notin C_\alpha$  then reject hypothesis that structure is an artifact with confidence  $(1 - \alpha)\%$ , *i.e.* **structure most likely physical**.
  - If  $\mathbf{x}' \in C_\alpha$  uncertainly too high to draw strong conclusions about the physical nature of the structure.

# Hypothesis testing

## Method

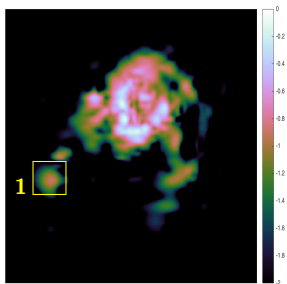
- Is structure in an image **physical or an artifact**?
- Perform **hypothesis tests** using Bayesian credible regions (Pereyra 2016b).
- Let  $C_\alpha$  denote the **highest posterior density (HPD) Bayesian credible region** with confidence level  $(1 - \alpha)\%$  defined by posterior iso-contour:  $C_\alpha = \{\mathbf{x} : g(\mathbf{x}) \leq \gamma_\alpha\}$ .

### Hypothesis testing of physical structure

- 1 Cut out region containing structure of interest from recovered image  $\mathbf{x}^*$ .
- 2 Inpaint background (noise) into region, yielding surrogate image  $\mathbf{x}'$ .
- 3 Test whether  $\mathbf{x}' \in C_\alpha$ :
  - If  $\mathbf{x}' \notin C_\alpha$  then reject hypothesis that structure is an artifact with confidence  $(1 - \alpha)\%$ , *i.e.* **structure most likely physical**.
  - If  $\mathbf{x}' \in C_\alpha$  uncertainty too high to draw strong conclusions about the physical nature of the structure.

# Hypothesis testing

## Numerical experiments



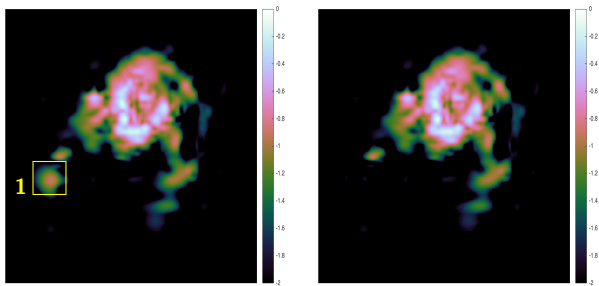
(a) Recovered image

Figure: HII region of M31



# Hypothesis testing

## Numerical experiments



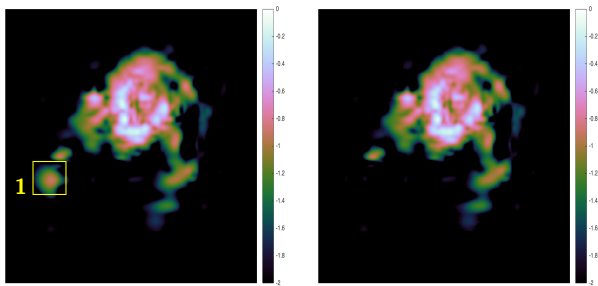
(a) Recovered image

(b) Surrogate with region removed

Figure: HII region of M31

# Hypothesis testing

## Numerical experiments



(a) Recovered image

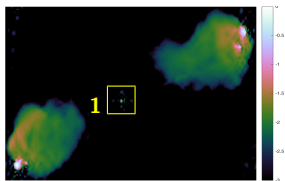
(b) Surrogate with region removed

1. Reject null hypothesis  
⇒ structure physical

Figure: HII region of M31

# Hypothesis testing

## Numerical experiments

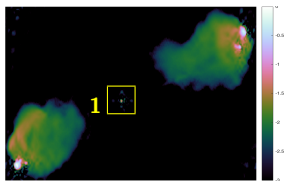


(a) Recovered image

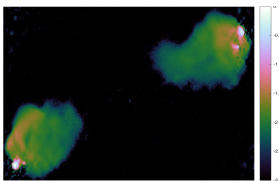
Figure: Cygnus A

# Hypothesis testing

## Numerical experiments



(a) Recovered image

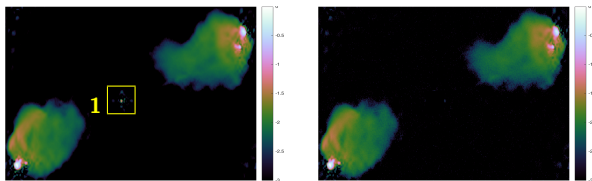


(b) Surrogate with region removed

Figure: Cygnus A

# Hypothesis testing

## Numerical experiments



(a) Recovered image

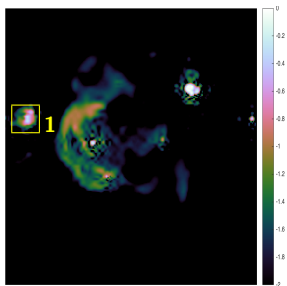
(b) Surrogate with region removed

Figure: Cygnus A

1. Cannot reject null hypothesis  
 $\Rightarrow$  cannot make strong statistical statement about origin of structure

# Hypothesis testing

## Numerical experiments

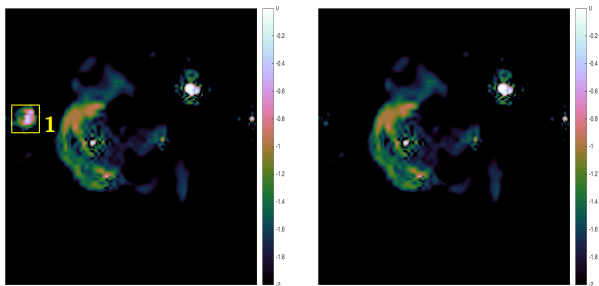


(a) Recovered image

Figure: Supernova remnant W28

# Hypothesis testing

## Numerical experiments



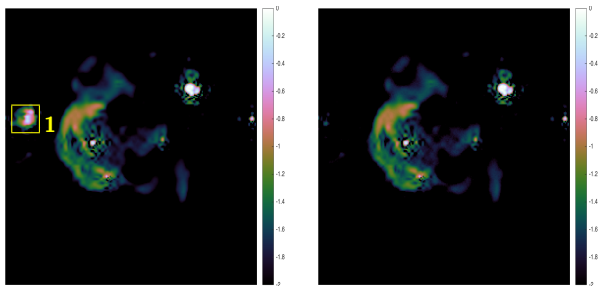
(a) Recovered image

(b) Surrogate with region removed

Figure: Supernova remnant W28

# Hypothesis testing

## Numerical experiments



(a) Recovered image

(b) Surrogate with region removed

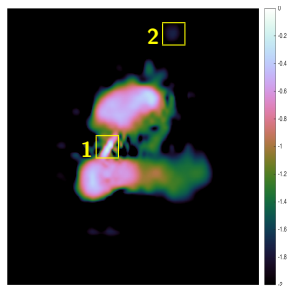
1. Reject null hypothesis  
⇒ structure physical

Figure: Supernova remnant W28



# Hypothesis testing

## Numerical experiments

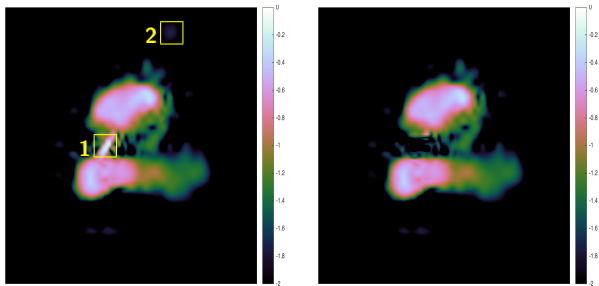


(a) Recovered image

Figure: 3C288

# Hypothesis testing

## Numerical experiments



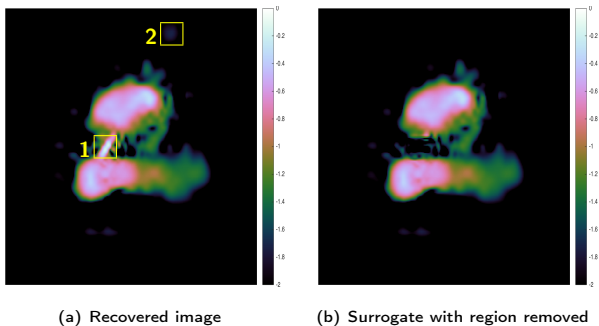
(a) Recovered image

(b) Surrogate with region removed

Figure: 3C288

# Hypothesis testing

## Numerical experiments



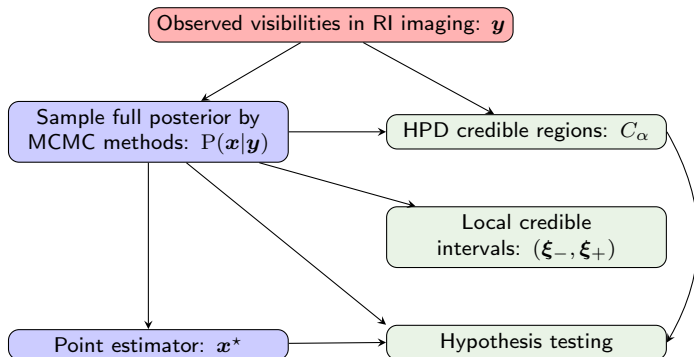
1. Reject null hypothesis  
⇒ structure physical
2. Cannot reject null hypothesis  
⇒ cannot make strong statistical statement about origin of structure

Figure: 3C288

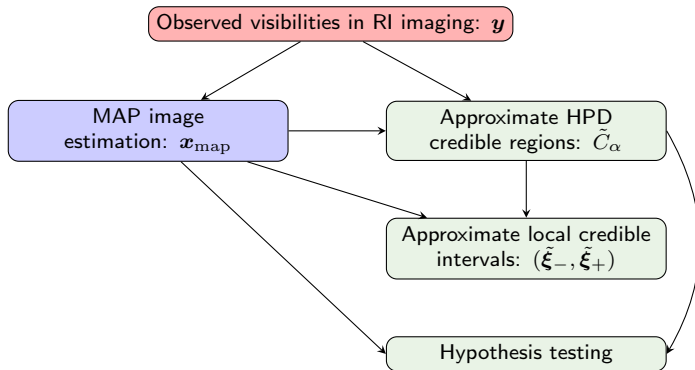
# Outline

- 1 Radio interferometric imaging
- 2 Proximal MCMC sampling and uncertainty quantification
  - Proximal Metropolis-adjusted Langevin algorithm (P-MALA)
  - Moreau-Yosida unadjusted Langevin algorithm (MYULA)
  - Numerical experiments
  - Hypothesis testing
- 3 MAP estimation and uncertainty quantification
  - Approximate local Bayesian credible intervals
  - Numerical experiments
  - Hypothesis testing

## Proximal MCMC sampling and uncertainty quantification



## MAP estimation and uncertainty quantification



## Approximate Bayesian credible regions for MAP estimation

- Combine **uncertainty quantification** with **fast sparse regularisation** to scale to big-data.
- Recall  $C_\alpha$  denotes the **highest posterior density (HPD) Bayesian credible region** with confidence level  $(1 - \alpha)\%$  defined by posterior iso-contour:  $C_\alpha = \{\mathbf{x} : g(\mathbf{x}) \leq \gamma_\alpha\}$ .
- Analytic approximation of  $\gamma_\alpha$ :

$$\tilde{\gamma}_\alpha = g(\mathbf{x}^*) + N(\tau_\alpha + 1)$$

where  $\tau_\alpha = \sqrt{16 \log(3/\alpha)/N}$  and  $\alpha \in (4\exp(-N/3), 1)$  (Pereyra 2016b). Follows by recent results from information theory, related to a concentration property of log-concave random vectors.

- Define **approximate HPD regions** by  $\tilde{C}_\alpha = \{\mathbf{x} : g(\mathbf{x}) \leq \tilde{\gamma}_\alpha\}$ .
- **Compute  $\mathbf{x}^*$**  by sparse regularisation, then **estimate local Bayesian credible intervals** and perform **hypothesis testing** using approximate HPD regions.

## Approximate Bayesian credible regions for MAP estimation

- Combine **uncertainty quantification** with **fast sparse regularisation** to scale to big-data.
- Recall  $C_\alpha$  denotes the **highest posterior density (HPD) Bayesian credible region** with confidence level  $(1 - \alpha)\%$  defined by posterior iso-contour:  $C_\alpha = \{\mathbf{x} : g(\mathbf{x}) \leq \gamma_\alpha\}$ .
- Analytic approximation of  $\gamma_\alpha$ :

$$\tilde{\gamma}_\alpha = g(\mathbf{x}^*) + N(\tau_\alpha + 1)$$

where  $\tau_\alpha = \sqrt{16 \log(3/\alpha)/N}$  and  $\alpha \in (4\exp(-N/3), 1)$  (Pereyra 2016b). Follows by recent results from information theory, related to a concentration property of log-concave random vectors.

- Define **approximate HPD regions** by  $\tilde{C}_\alpha = \{\mathbf{x} : g(\mathbf{x}) \leq \tilde{\gamma}_\alpha\}$ .
- **Compute  $\mathbf{x}^*$**  by sparse regularisation, then **estimate local Bayesian credible intervals** and perform **hypothesis testing** using approximate HPD regions.



## Approximate Bayesian credible regions for MAP estimation

- Combine **uncertainty quantification** with **fast sparse regularisation** to scale to big-data.
- Recall  $C_\alpha$  denotes the **highest posterior density (HPD) Bayesian credible region** with confidence level  $(1 - \alpha)\%$  defined by posterior iso-contour:  $C_\alpha = \{\mathbf{x} : g(\mathbf{x}) \leq \gamma_\alpha\}$ .
- **Analytic approximation** of  $\gamma_\alpha$ :

$$\tilde{\gamma}_\alpha = g(\mathbf{x}^*) + N(\tau_\alpha + 1)$$

where  $\tau_\alpha = \sqrt{16 \log(3/\alpha)/N}$  and  $\alpha \in (4\exp(-N/3), 1)$  (Pereyra 2016b). Follows by recent results from information theory, related to a concentration property of log-concave random vectors.

- Define **approximate HPD regions** by  $\tilde{C}_\alpha = \{\mathbf{x} : g(\mathbf{x}) \leq \tilde{\gamma}_\alpha\}$ .
- **Compute  $\mathbf{x}^*$**  by sparse regularisation, then **estimate local Bayesian credible intervals** and perform **hypothesis testing** using approximate HPD regions.

## Approximate Bayesian credible regions for MAP estimation

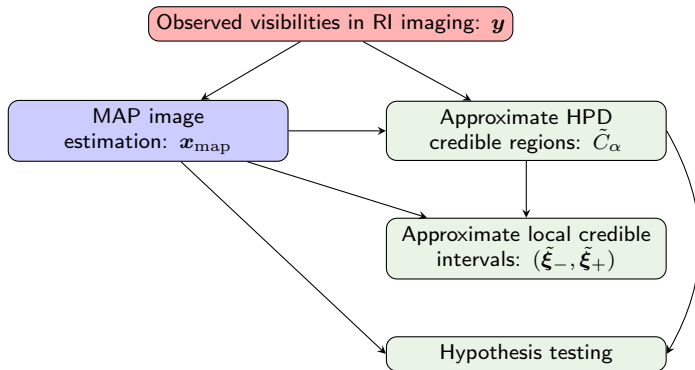
- Combine **uncertainty quantification** with **fast sparse regularisation** to scale to big-data.
- Recall  $C_\alpha$  denotes the **highest posterior density (HPD) Bayesian credible region** with confidence level  $(1 - \alpha)\%$  defined by posterior iso-contour:  $C_\alpha = \{\mathbf{x} : g(\mathbf{x}) \leq \gamma_\alpha\}$ .
- **Analytic approximation** of  $\gamma_\alpha$ :

$$\tilde{\gamma}_\alpha = g(\mathbf{x}^*) + N(\tau_\alpha + 1)$$

where  $\tau_\alpha = \sqrt{16 \log(3/\alpha)/N}$  and  $\alpha \in (4\exp(-N/3), 1)$  (Pereyra 2016b). Follows by recent results from information theory, related to a concentration property of log-concave random vectors.

- Define **approximate HPD regions** by  $\tilde{C}_\alpha = \{\mathbf{x} : g(\mathbf{x}) \leq \tilde{\gamma}_\alpha\}$ .
- **Compute  $\mathbf{x}^*$**  by sparse regularisation, then **estimate local Bayesian credible intervals** and perform **hypothesis testing** using approximate HPD regions.

## MAP estimation and uncertainty quantification



# Local Bayesian credible intervals for MAP estimation

## Local Bayesian credible intervals for sparse reconstruction

(Cai, Pereyra & McEwen, in prep.)

Let  $\Omega$  define the area (or pixel) over which to compute the credible interval  $(\tilde{\xi}_-, \tilde{\xi}_+)$  and  $\zeta$  be an index vector describing  $\Omega$  (i.e.  $\zeta_i = 1$  if  $i \in \Omega$  and 0 otherwise).

Given  $\tilde{\gamma}_\alpha$  and  $\mathbf{x}^*$ , compute the credible interval by

$$\begin{aligned}\tilde{\xi}_- &= \min_{\xi} \{ \xi \mid g_{\mathbf{y}}(\mathbf{x}') \leq \tilde{\gamma}_\alpha, \forall \xi \in [-\infty, +\infty) \}, \\ \tilde{\xi}_+ &= \max_{\xi} \{ \xi \mid g_{\mathbf{y}}(\mathbf{x}') \leq \tilde{\gamma}_\alpha, \forall \xi \in [-\infty, +\infty) \},\end{aligned}$$

where

$$\mathbf{x}' = \mathbf{x}^*(\mathcal{I} - \zeta) + \xi\zeta.$$

# Numerical experiments

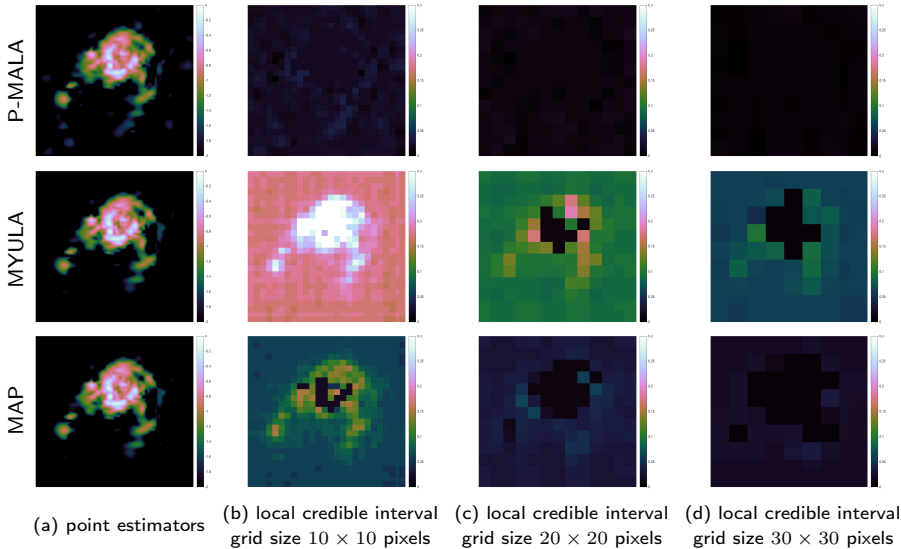
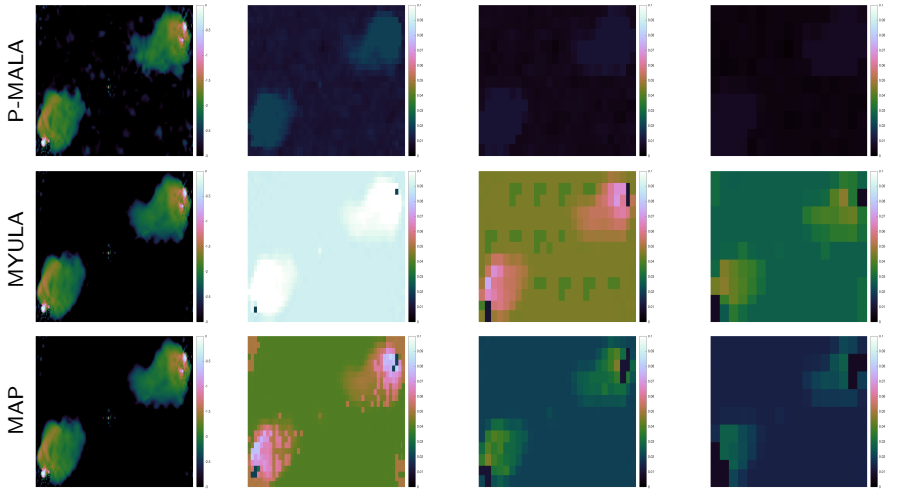


Figure: Local credible interval computation for M31 for the analysis model.

# Numerical experiments



(a) point estimators      (b) local credible interval grid size  $10 \times 10$  pixels      (c) local credible interval grid size  $20 \times 20$  pixels      (d) local credible interval grid size  $30 \times 30$  pixels

Figure: Local credible interval computation for Cygnus A for the analysis model.

# Numerical experiments

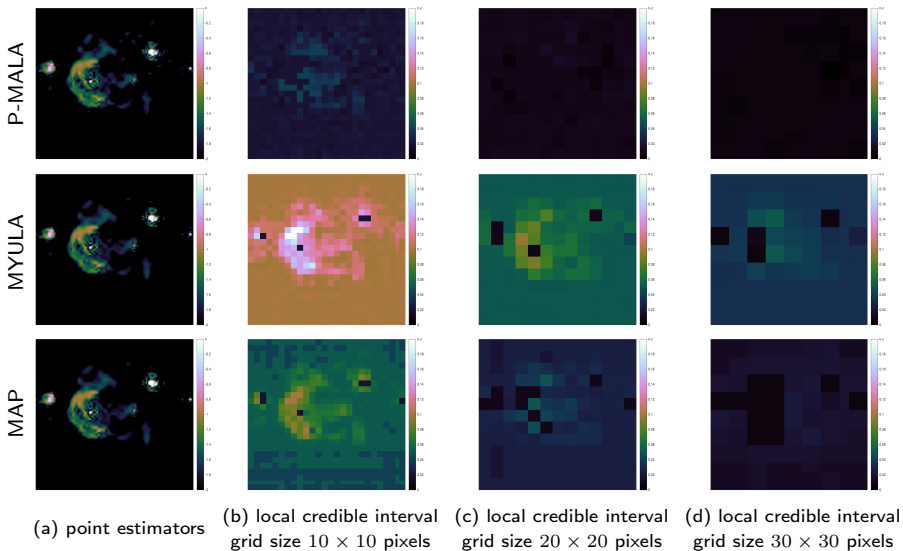


Figure: Local credible interval computation for W28 for the analysis model.

# Numerical experiments

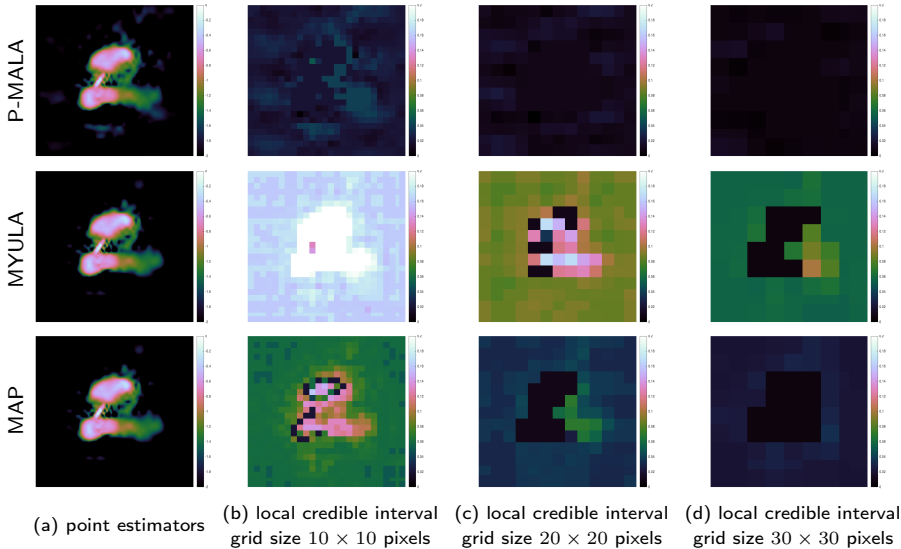


Figure: Local credible interval computation for 3C288 for the analysis model.



# Numerical experiments

## Computation time

Table: CPU time in minutes for Proximal MCMC sampling and MAP estimation

Image	Method	CPU time	
		Analysis	Synthesis
Cygnus A	P-MALA	2274	1762
	MYULA	1056	942
	MAP	.07	.04
M31	P-MALA	1307	944
	MYULA	618	581
	MAP	.03	.02
W28	P-MALA	1122	879
	MYULA	646	598
	MAP	.06	.04
3C288	P-MALA	1144	881
	MYULA	607	538
	MAP	.03	.02

# Hypothesis testing

## Comparison of numerical experiments

Table: Comparison of hypothesis tests for different methods for the analysis model.

Image	Test area	Ground truth	Method	Hypothesis test
M31	1	✓	P-MALA	✓
			MYULA	✓
			MAP	✓
Cygnus A	1	✓	P-MALA	✗
			MYULA*	✗
			MAP	✗
W28	1	✓	P-MALA	✓
			MYULA	✓
			MAP	✓
3C288	1	✓	P-MALA	✓
			MYULA	✓
			MAP	✓
	2	✗	P-MALA	✗
			MYULA	✗
			MAP	✗

(\* Can correctly detect physical structure if use median point estimator.)

## Conclusions

- 1 **Sparse priors** shown to be **highly effective** and **scalable** to big-data.  
PURIFY package provides robust framework for imaging interferometric observations (<http://basp-group.github.io/purify/>).
- 2 **Proximal MCMC** sampling can support sparse priors in full **Bayesian** framework:
  - Recover Bayesian credible intervals.
  - Perform hypothesis testing to test whether structure physical.
- 3 **MAP estimation** (sparse regularisation) with approximate uncertainty quantification:
  - Recover Bayesian credible intervals.
  - Perform hypothesis testing to test whether structure physical.

Scalable to big-data (computational time saving  $\gg 10^5$ )

Supported by:



## Conclusions

- 1 **Sparse priors** shown to be **highly effective** and **scalable** to big-data.  
PURIFY package provides robust framework for imaging interferometric observations (<http://basp-group.github.io/purify/>).
- 2 **Proximal MCMC** sampling can support sparse priors in full **Bayesian** framework:
  - Recover **Bayesian credible intervals**.
  - Perform **hypothesis testing** to test whether structure physical.
- 3 **MAP estimation (sparse regularisation)** with **approximate uncertainty quantification**:
  - Recover **Bayesian credible intervals**.
  - Perform **hypothesis testing** to test whether structure physical.

Scalable to big-data (computational time saving  $\gg 10^5$ )

Supported by:



# Conclusions

- 1 **Sparse priors** shown to be **highly effective** and **scalable** to big-data.  
PURIFY package provides robust framework for imaging interferometric observations (<http://basp-group.github.io/purify/>).
- 2 **Proximal MCMC** sampling can support sparse priors in full **Bayesian** framework:
  - Recover **Bayesian credible intervals**.
  - Perform **hypothesis testing** to test whether structure physical.
- 3 **MAP estimation (sparse regularisation)** with **approximate uncertainty quantification**:
  - Recover **Bayesian credible intervals**.
  - Perform **hypothesis testing** to test whether structure physical.

Scalable to big-data (computational time saving  $\gg 10^5$ )

Supported by:

# Extra Slides

Analysis vs synthesis

Bayesian interpretations

Distribution and parallelisation

PURIFY reconstructions

# Extra Slides

Analysis vs synthesis

## Analysis vs synthesis

- Typically sparsity assumption is justified by analysing example signals in terms of atoms of the dictionary.
- Different to synthesising signals from atoms.
- Suggests an **analysis-based** framework (Elad *et al.* 2007, Nam *et al.* 2012):

$$\mathbf{x}^* = \arg \min_{\mathbf{x}} \|\Omega \mathbf{x}\|_1 \text{ subject to } \|\mathbf{y} - \Phi \mathbf{x}\|_2 \leq \epsilon .$$

analysis

- Contrast with **synthesis-based** approach:

$$\mathbf{x}^* = \Psi \cdot \arg \min_{\alpha} \|\alpha\|_1 \text{ subject to } \|\mathbf{y} - \Phi \Psi \alpha\|_2 \leq \epsilon .$$

synthesis

- For **orthogonal bases**  $\Omega = \Psi^\dagger$  and the two approaches are **identical**.



# Analysis vs synthesis

## Comparison

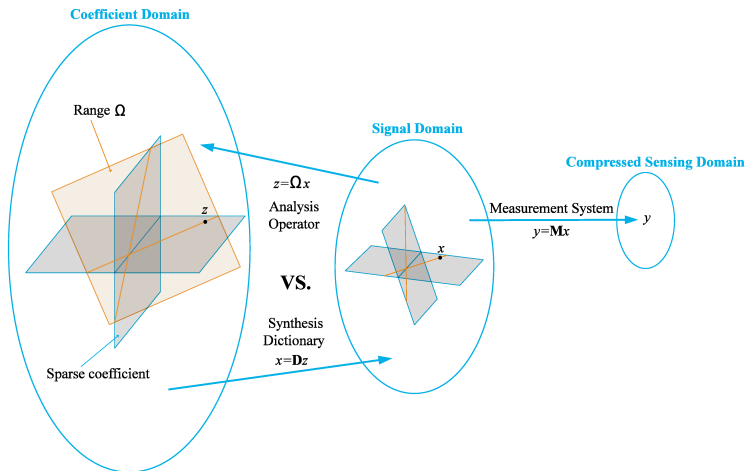


Figure: Analysis- and synthesis-based approaches [Credit: Nam et al. (2012)].

# Analysis vs synthesis

## Comparison

- Synthesis-based approach is more general, while analysis-based approach more restrictive.
- More restrictive analysis-based approach may make it more robust to noise.
- The greater descriptive power of the synthesis-based approach may provide better signal representations (too descriptive?).

# Extra Slides

Bayesian interpretations

## Bayesian interpretations

### One Bayesian interpretation of the synthesis-based approach

- Consider the inverse problem:

$$\mathbf{y} = \Phi\Psi\boldsymbol{\alpha} + \mathbf{n}.$$

- Assume Gaussian noise, yielding the likelihood:

$$P(\mathbf{y} | \boldsymbol{\alpha}) \propto \exp\left(-\frac{\|\mathbf{y} - \Phi\Psi\boldsymbol{\alpha}\|_2^2}{2\sigma^2}\right).$$

- Consider the Laplacian prior:

$$P(\boldsymbol{\alpha}) \propto \exp\left(-\beta\|\boldsymbol{\alpha}\|_1\right).$$

- The **maximum *a-posteriori* (MAP) estimate** (with  $\lambda = 2\beta\sigma^2$ ) is

$$\mathbf{x}_{\text{MAP-synthesis}}^* = \Psi \cdot \arg \max_{\boldsymbol{\alpha}} P(\boldsymbol{\alpha} | \mathbf{y}) = \Psi \cdot \arg \min_{\boldsymbol{\alpha}} \|\mathbf{y} - \Phi\Psi\boldsymbol{\alpha}\|_2^2 + \lambda\|\boldsymbol{\alpha}\|_1.$$

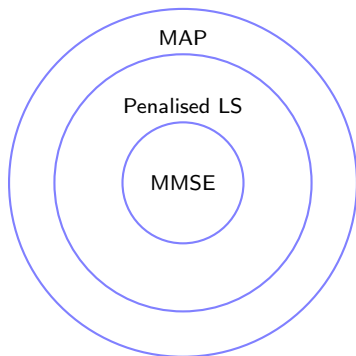
synthesis

- One** possible Bayesian interpretation!
- Signal may be  $\ell_0$ -sparse**, then solving  $\ell_1$  problem finds the correct  $\ell_0$ -sparse solution!

# Bayesian interpretations

## Other Bayesian interpretations of the synthesis-based approach

- Other Bayesian interpretations are also possible (Gribonval 2011).
- Minimum mean square error (MMSE) estimators
  - synthesis-based estimators with appropriate penalty function, *i.e.* penalised least-squares (LS)
  - MAP estimators



## Bayesian interpretations

### One Bayesian interpretation of the analysis-based approach

- Analysis-based MAP estimate is

$$\mathbf{x}_{\text{MAP-analysis}}^* = \Omega^\dagger \cdot \arg \min_{\gamma \in \text{column space } \Omega} \|\mathbf{y} - \Phi \Omega^\dagger \gamma\|_2^2 + \lambda \|\gamma\|_1.$$

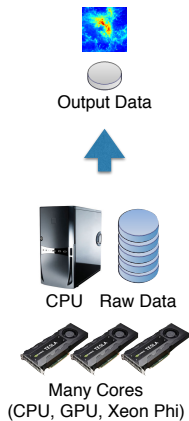
analysis

- Different to synthesis-based approach if analysis operator  $\Omega$  is not an orthogonal basis.
- Analysis-based approach **more restrictive** than synthesis-based.
- Similar ideas promoted by Maisinger, Hobson & Lasenby (2004) in a Bayesian framework for wavelet MEM (maximum entropy method).

# Extra Slides

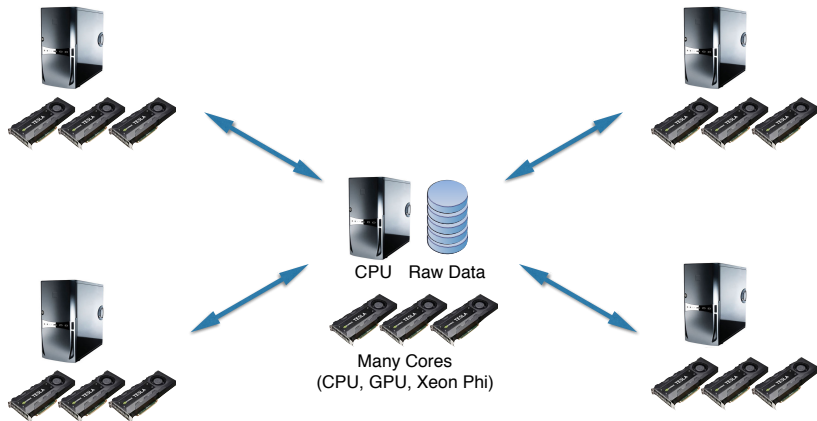
Distribution and parallelisation

# Standard algorithms

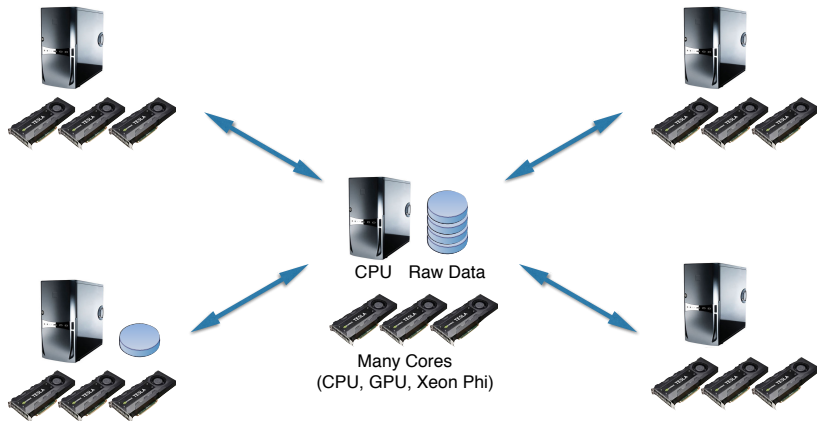




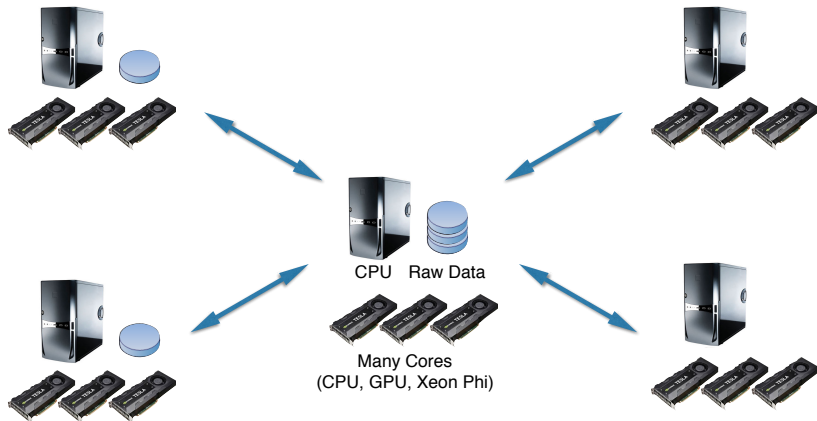
# Highly distributed and parallelised algorithms



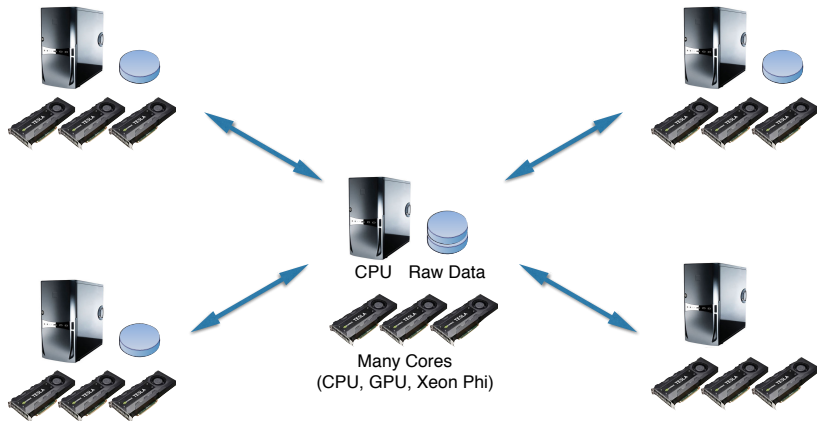
# Highly distributed and parallelised algorithms



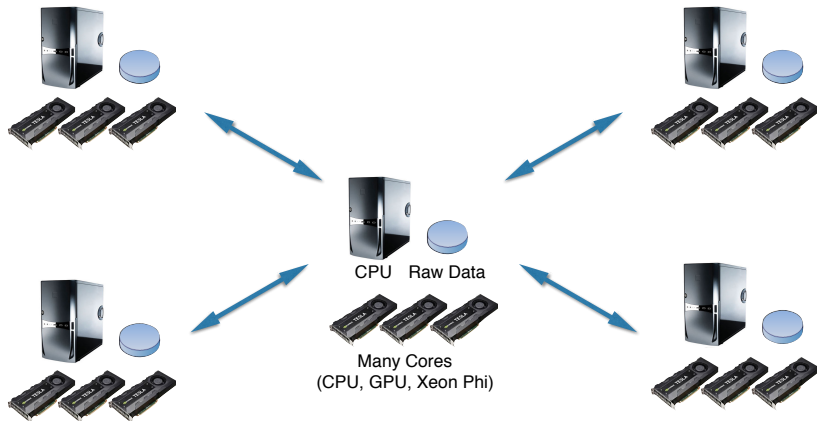
# Highly distributed and parallelised algorithms



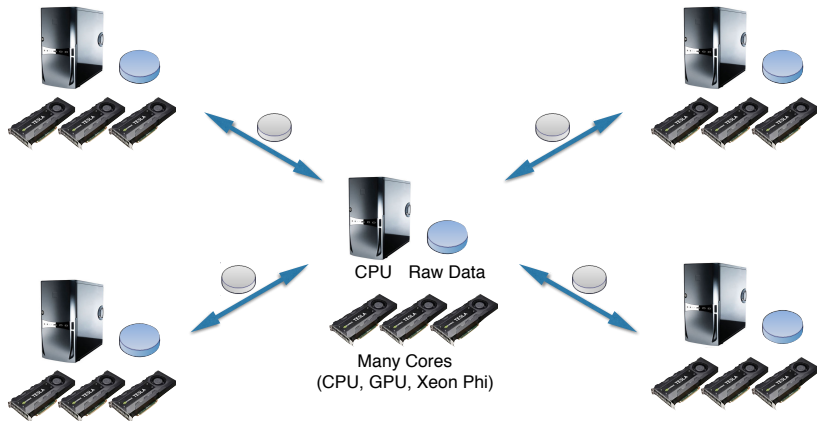
# Highly distributed and parallelised algorithms



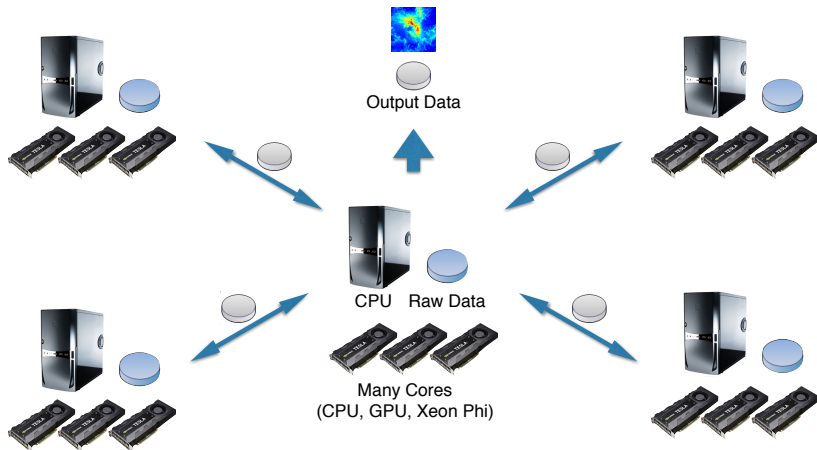
# Highly distributed and parallelised algorithms



# Highly distributed and parallelised algorithms



# Highly distributed and parallelised algorithms



# Extra Slides

PURIFY reconstructions



# PURIFY reconstruction

## VLA observation of 3C129

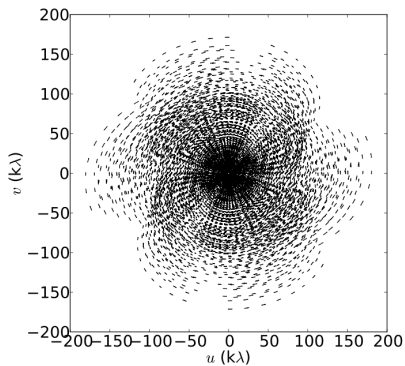


Figure: VLA visibility coverage for 3C129

## PURIFY reconstruction

VLA observation of 3C129

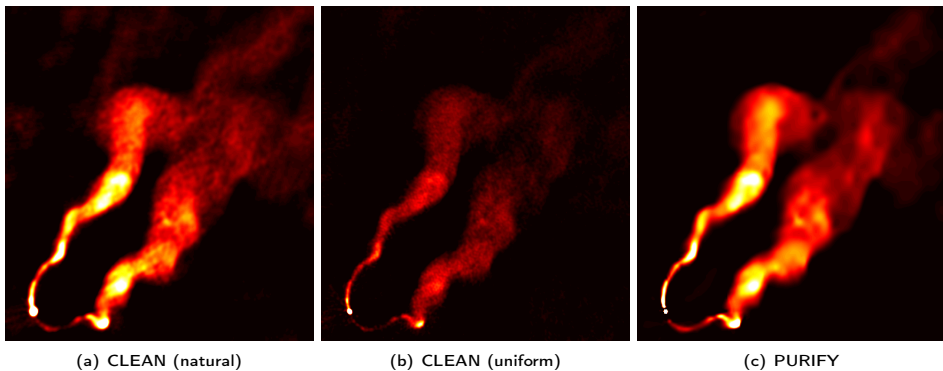
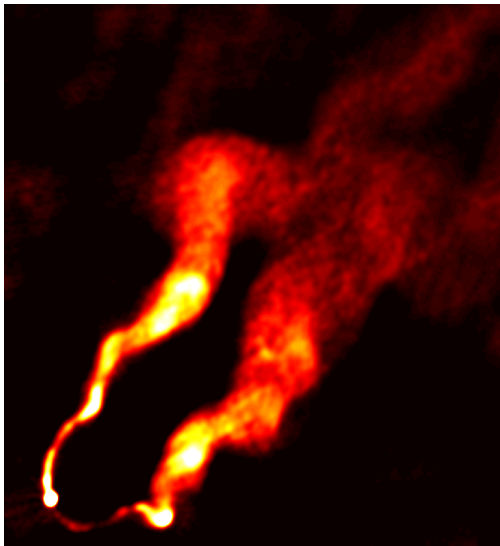


Figure: 3C129 recovered images (Pratley, McEwen, et al. 2016)

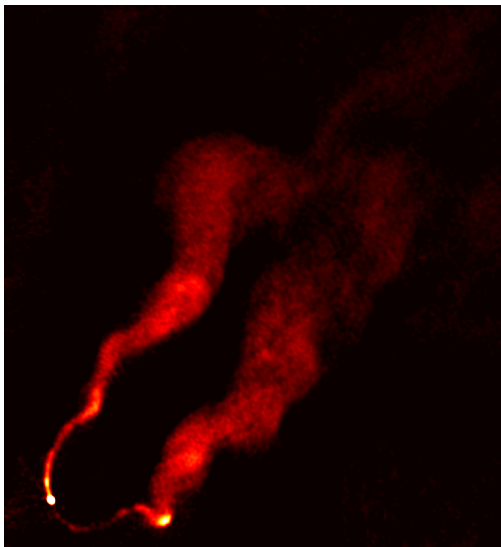
# PURIFY reconstruction

VLA observation of 3C129 imaged by CLEAN (natural)



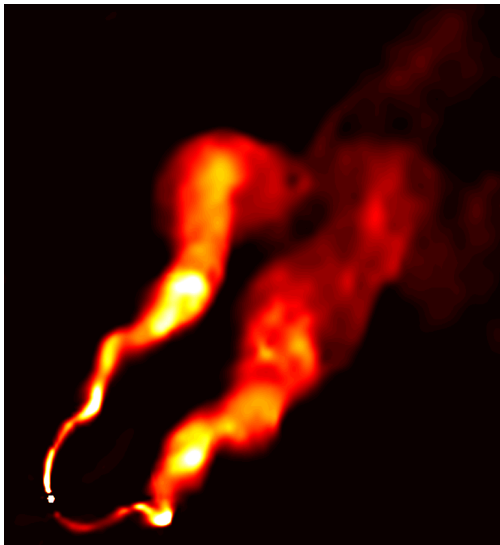
# PURIFY reconstruction

VLA observation of 3C129 images by CLEAN (uniform)



# PURIFY reconstruction

VLA observation of 3C129 images by PURIFY



# PURIFY reconstruction

## VLA observation of 3C129

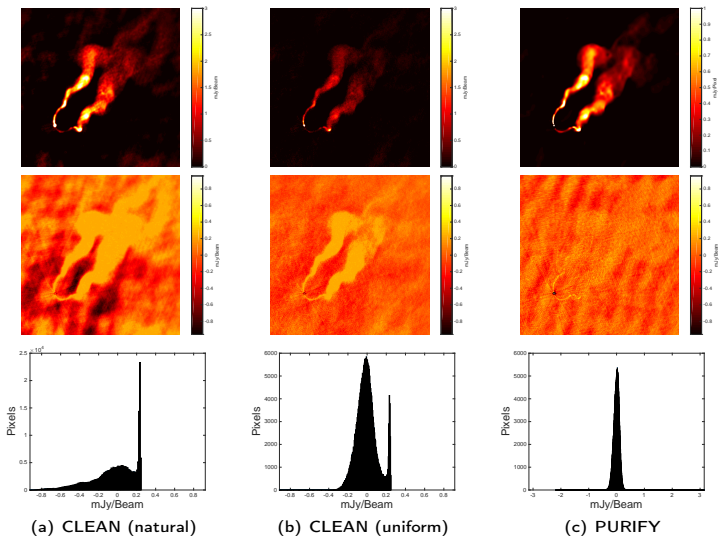


Figure: 3C129 recovered images and residuals (Pratley, McEwen, *et al.* 2016)

# PURIFY reconstruction

## VLA observation of Cygnus A

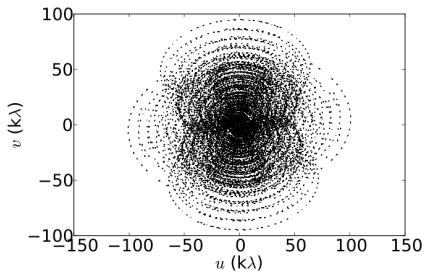


Figure: VLA visibility coverage for Cygnus A

# PURIFY reconstruction

## VLA observation of Cygnus A

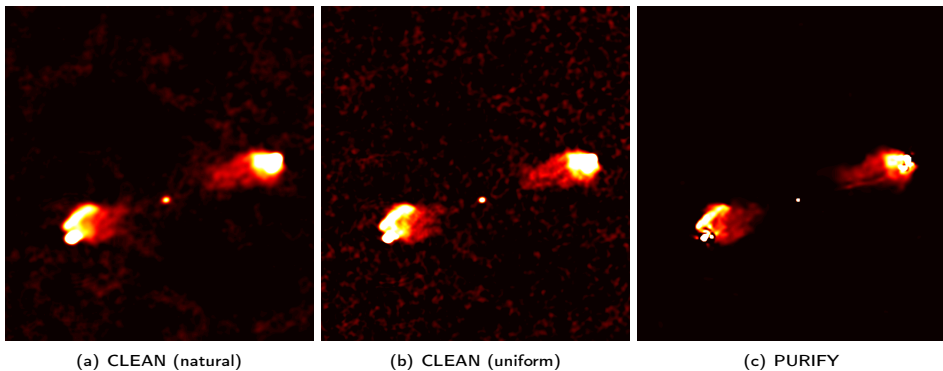
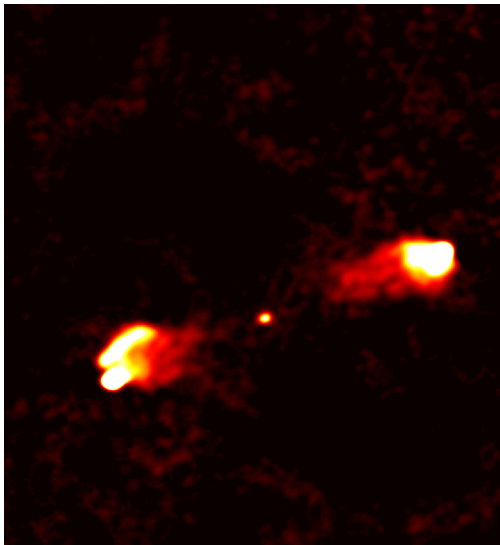


Figure: Cygnus A recovered images (Pratley, McEwen, *et al.* 2016)



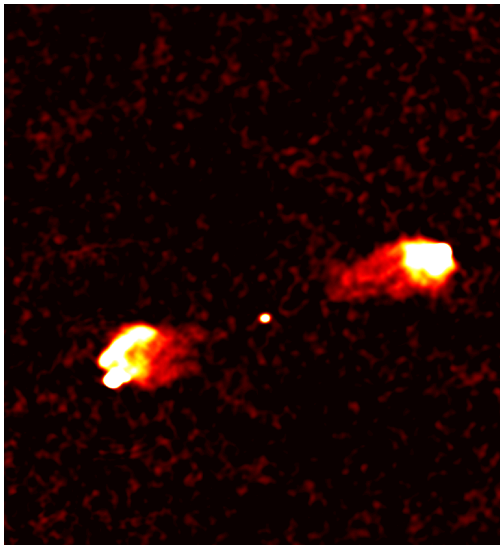
# PURIFY reconstruction

VLA observation of Cygnus A imaged by CLEAN (natural)



# PURIFY reconstruction

VLA observation of Cygnus A images by CLEAN (uniform)



# PURIFY reconstruction

VLA observation of Cygnus A images by PURIFY



# PURIFY reconstruction

## VLA observation of Cygnus A

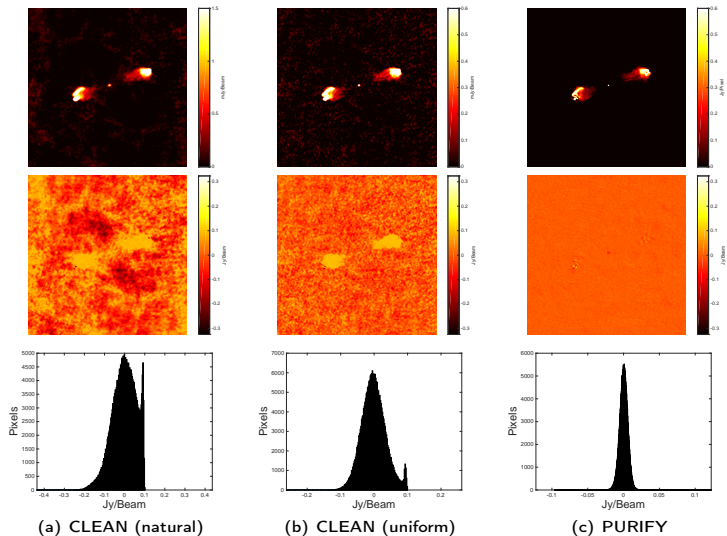


Figure: Cygnus A recovered images and residuals (Pratley, McEwen, *et al.* 2016)

## PURIFY reconstruction

ATCA observation of PKS J0334-39

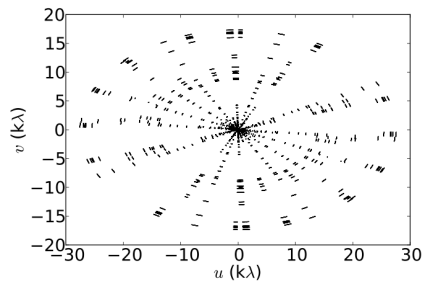


Figure: VLA visibility coverage for PKS J0334-39

## PURIFY reconstruction

ATCA observation of PKS J0334-39

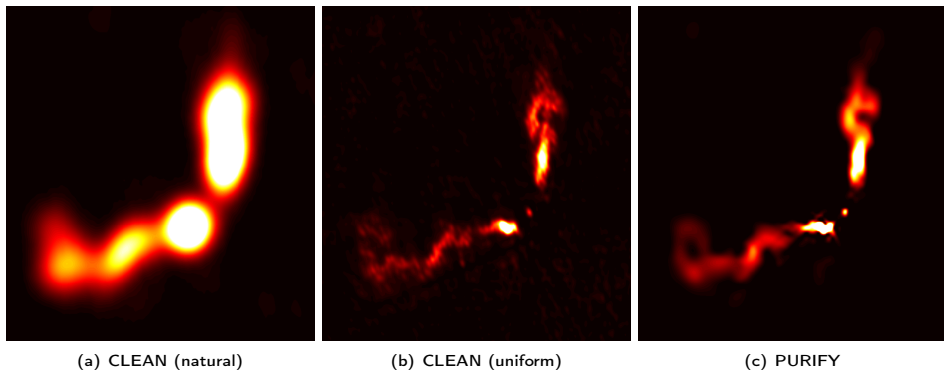
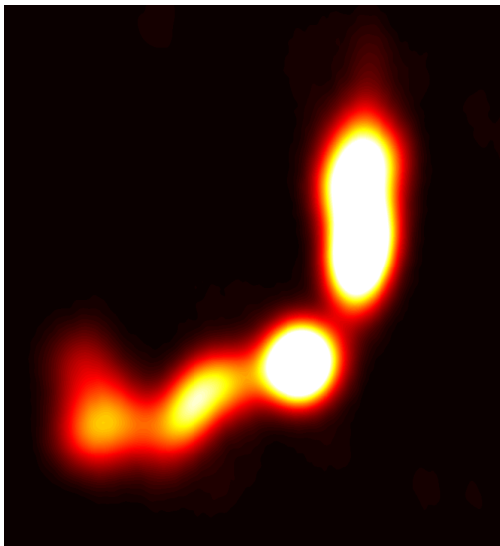


Figure: PKS J0334-39 recovered images (Pratley, McEwen, et al. 2016)

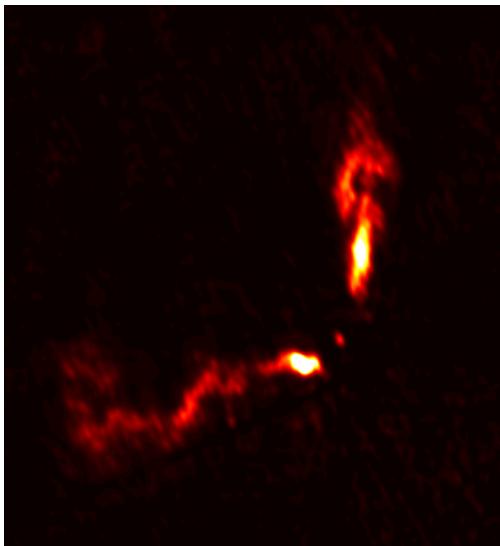
## PURIFY reconstruction

VLA observation of PKS J0334-39 imaged by CLEAN (natural)



## PURIFY reconstruction

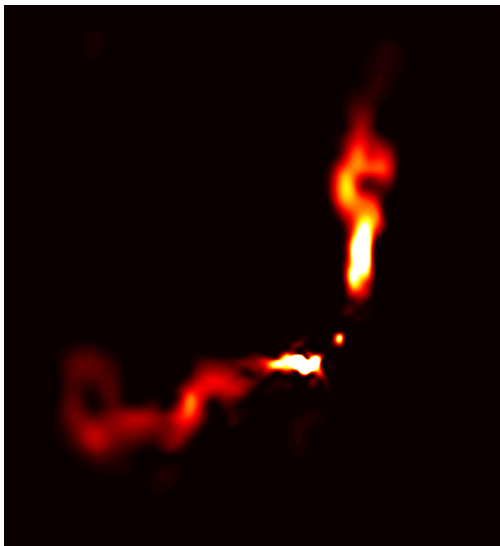
VLA observation of PKS J0334-39 images by CLEAN (uniform)





## PURIFY reconstruction

VLA observation of PKS J0334-39 images by PURIFY



## PURIFY reconstruction

ATCA observation of PKS J0334-39

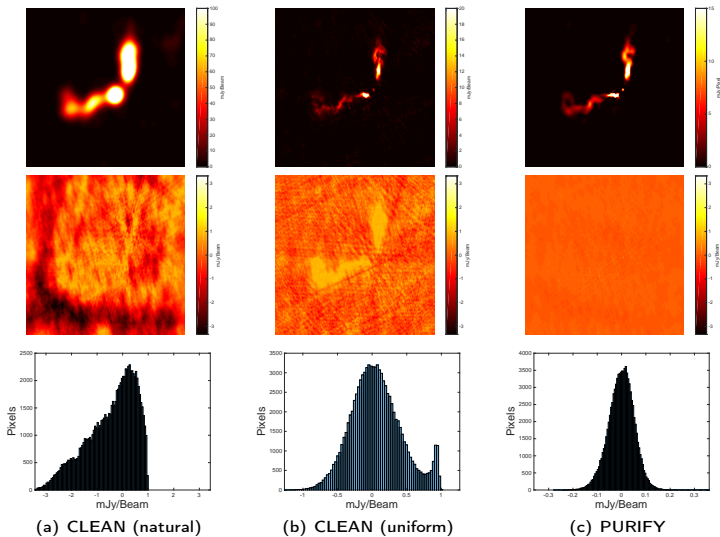


Figure: PKS J0334-39 recovered images and residuals (Pratley, McEwen, *et al.* 2016)

## PURIFY reconstruction

ATCA observation of PKS J0116-473

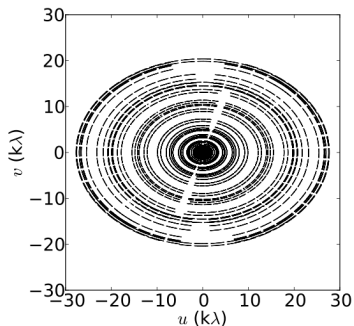


Figure: ATCA visibility coverage for Cygnus A

## PURIFY reconstruction

ATCA observation of PKS J0116-473

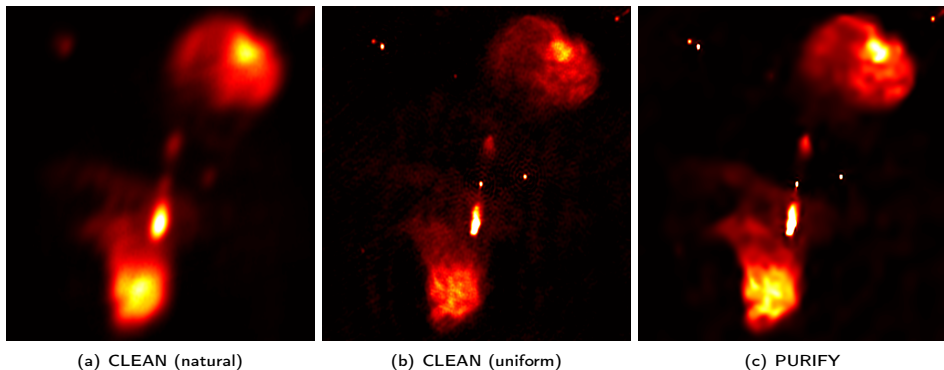
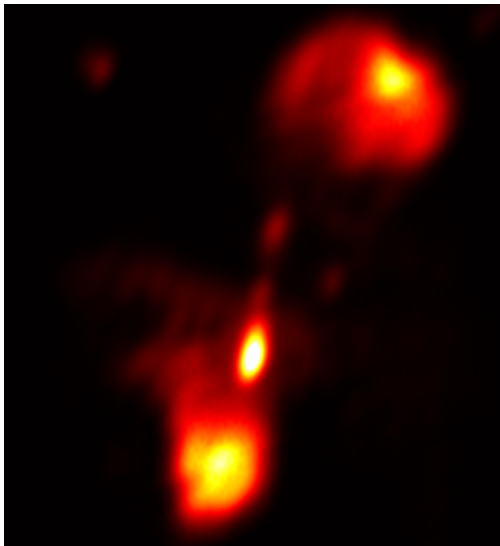


Figure: PKS J0116-473 recovered images (Pratley, McEwen, *et al.* 2016)

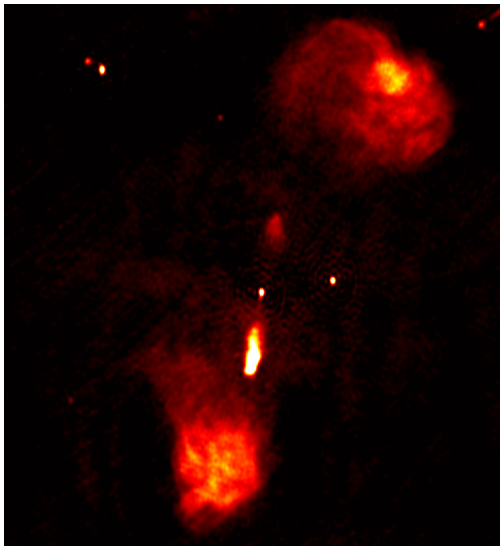
## PURIFY reconstruction

VLA observation of PKS J0116-473 imaged by CLEAN (natural)



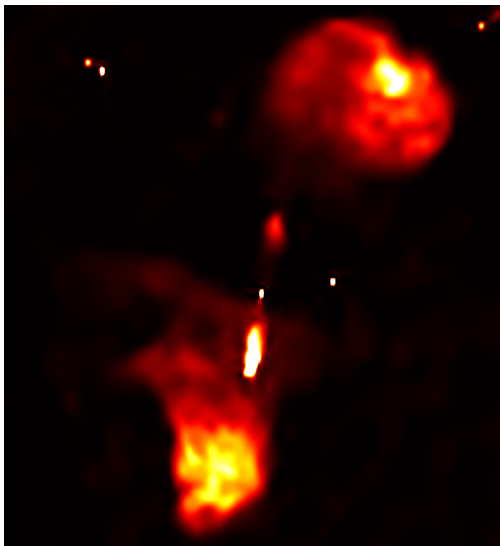
## PURIFY reconstruction

VLA observation of PKS J0116-473 images by CLEAN (uniform)



# PURIFY reconstruction

VLA observation of PKS J0116-473 images by PURIFY



## PURIFY reconstruction

ATCA observation of PKS J0116-473

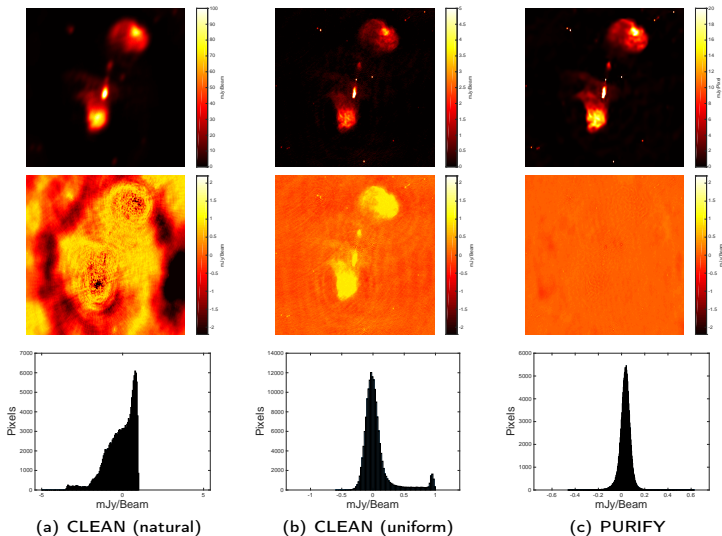


Figure: PKS J0116-473 recovered images and residuals (Pratley, McEwen, *et al.* 2016)



## PURIFY reconstructions

Table: Root-mean-square of residuals of each reconstruction (units in mJy/Beam)

Observation	PURIFY	CLEAN (natural)	CLEAN (uniform)
3C129	0.10	0.23	0.11
Cygnus A	6.1	59	36
PKS J0334-39	0.052	1.00	0.37
PKS J0116-473	0.054	0.88	0.24